CHALMERS
UNIVERSITY OF TECHNOLOGY

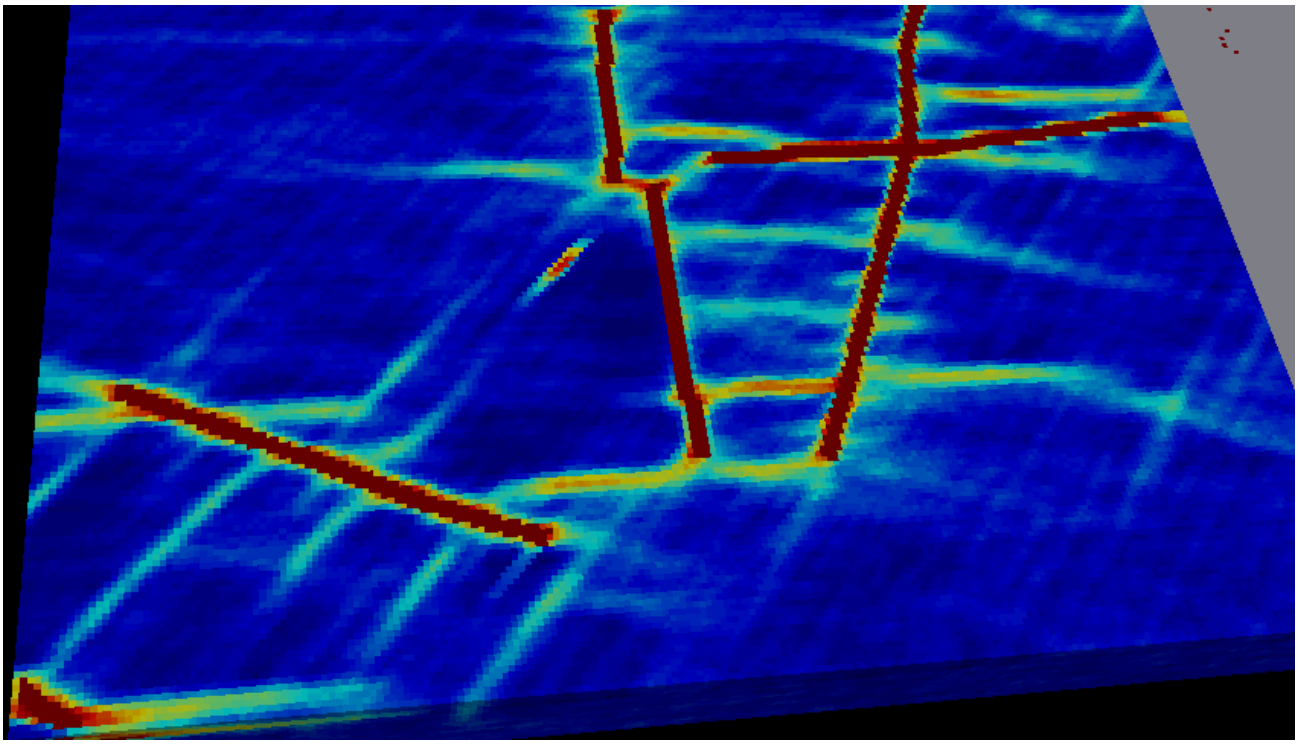

The value of information of deformation zones in bedrock for grouting design

Master's thesis in Infrastructure and Environmental Engineering

WILLIAM ELIASSON

MARTIN THORSSON

DEPARTMENT OF ARCHITECTURE AND CIVIL ENGINEERING

CHALMERS UNIVERSITY OF TECHNOLOGY
Gothenburg, Sweden 2024
www.chalmers.se

MASTER'S THESIS 2024

The value of information of deformation zones in bedrock for grouting design

WILLIAM ELIASSON
MARTIN THORSSON

CHALMERS
UNIVERSITY OF TECHNOLOGY

Department of Architecture and Civil Engineering
Division of Geology and Geotechnics
Engineering Geology
CHALMERS UNIVERSITY OF TECHNOLOGY
Gothenburg, Sweden 2024

The value of information of deformation zones in bedrock for grouting design
WILLIAM ELIASSON
MARTIN THORSSON

Supervisors: Johanna Meriaslu, Department of Geology and Geotechnics
Andreas Berg, COWI AB

Examiner: Lars Rosén, Department of Geology and Geotechnics

Master's Thesis 2024
Department of Geology and Geotechnics
Division of Architecture and Civil Engineering
Engineering Geology
Chalmers University of Technology
SE-412 96 Gothenburg
Telephone +46 31 772 1000

Cover: A probability-based geostatistical model of the deformation zone network in the area of Kolmårdstunneln, created in the software SGeMS.

Gothenburg, Sweden 2024

Abstract

Understanding of site-specific geological characteristics is of high importance in underground construction. In tunnelling, consideration must be given to possible modes of water transport in the rock since leakage could result in significant consequences for nearby nature and construction. Core drilling techniques are often utilized to characterize rock masses, but these are expensive and only give information specific to a given point of sampling. Hence, a balance must be maintained between the economical cost of conducting these investigations and the benefit they provide in terms of information. The aim of this project is to exemplify a methodology of applying Multiple point statistics (MPS) and Value of information analysis (VOIA) to evaluate the value of performing further core drilling investigations in a tunnelling project for the purpose of grouting design. This methodology has been showcased through application on the on-going tunnelling project Kolmårdstunneln, which is part of the bigger project Ostlänken, Sweden. The MPS algorithm SNESIM was used in the SGeMS software to construct a geostatistical model, whereafter two different grouting designs (A1 and A2) were evaluated using VOIA and compared in terms of their respective construction costs and their associated risk of failure- represented as the expected economic consequence for underestimating the occurrence of deformation zones in the tunnel. This evaluation comprised of two stages; a prior analysis which features a probability of failure dependent on the modelled rock mass in the tunnel, and a pre-posterior analysis, where the probability of failure has been adjusted using a virtual core drilling campaign and Bayesian updating. For the context of this case study, the value of information of a campaign was calculated by comparing the prior and pre-posterior results. It could be concluded that the campaign was not worth conducting since conducting the campaign would not have led to a different decision being made. The proposed method shows potential, but further research is necessary regarding several aspects.

Keywords: Multiple point statistics, Geostatistical modelling, SNESIM, SGeMS, Value of information analysis, Cost-benefit analysis, Deformation zones, Bayesian updating

Contents

1. Introduction

The evaluation of uncertainty plays a key role in any project related to underground construction. Uncertainty comes in different forms- aleatory uncertainty refers to the inherent randomness and variability in data, while epistemic uncertainty refers to the uncertainty found in any model used to describe reality and comes from a lack of knowledge of fundamental phenomena (Aven, 2003). Epistemic uncertainty can always be reduced by collecting more data, but in the context of underground construction, core drilling investigations done for the purposes of collecting this data can extract a significant toll economically (Monicard, 1980). Furthermore, data collected will always be specific to that very point location of collection and hence, it is necessary to adapt different methods to make broad interpretations in between points of data when characterizing a rock or soil mass (Davis et al., 2002).

Understanding of site-specific geological conditions is crucial for many engineering purposes. Since collecting data regarding the subsurface is both expensive and technically challenging, strategic sampling and economic considerations are of great importance in the execution of any underground construction. In the case of tunnelling, information regarding water bearing deformation zones plays a key role in determining the choice of grouting techniques used along the tunnel (Grøv & Woldmo, 2012), as leakage-induced drawdown of the groundwater table might cause severe consequences to surrounding nature and construction. Areas may be sensitive for different reasons, some issues relate to settlements that may cause damage to buildings and infrastructure, others to risks of harming sensitive natural values and ecosystems. During the last decades, new, more advanced geostatistical methods have made it possible to predict locations of unobserved deformation zones based on structural patterns in the bedrock (Tahmasebi, 2018). Utilizing these prediction techniques provides further information for decision-makers, hence allowing for further improvement of the sampling and pre-investigation planning.

In underground construction projects, there is a desire to reduce geological uncertainty while minimizing the investigation costs- presenting an optimization problem where finding a balance between uncertainty and costs of investigation is difficult (Freeze et al., 1992). An important means of handling and quantifying uncertainty in a geological setting is by means of geostatistical modelling. By making use of (discrete) information from investigations such as core-drilling campaigns, statistical models of the rock or soil can be constructed to better understand and visualize the possible variations in (continuous) space through interpolation (Davis et al., 2002). Commonly used methods of spatial interpolation include Kriging or Inverse-distance weighting (IDW), but since these methods are limited in their efficacy in constructing more complex geological patterns it is of interest to investigate new methods capable of reconstructing said complexities (Tahmasebi, 2018). Multiple point statistics (MPS) refers to algorithms that unlike the conventional Kriging method make use of multiple data points at a time to allow for this (Strebelle & Journel, 2001).

An important factor of consideration for any investigation is that if the cost of performing the measurements is higher than the value of the information gained, then the investigation is not worth performing (Freeze et al., 1992). Within decision-making analysis, a method of growing interest in the field of civil engineering is Value of information analysis (VOIA), which could prove to be a useful tool in regard to determining how many measurements ought to be taken within the context of a given project in order to maximize economic value (Freeze et al., 1992). For VOIA to be conducted in an engineering geological context, a geostatistical model is to be built. Multiple point statistics could provide valuable input as a means of constructing the geostatistical model needed in this context, as

their ability to describe complexities make them suitable for the simulation of deformation zones and fracture networks that are responsible for water transfer in crystalline rock.

1.1. Aim, objectives and limitations

This project aims to exemplify a method of combining geostatistical simulation using MPS and VOIA as a decision support for pre-investigations. The pre-investigations considered are core drillings, and their purpose is to identify permeable water bearing features along a tunnel. The value of new information from core drilling tests will be compared to the cost of sampling the same data. Application of the method will be illustrated with a case study constituting a tunnel in crystalline rocks where different alternative grouting designs are compared and evaluated.

Two alternative grouting designs are to be analysed. The difference between them is in their number of expected permeable water-bearing deformation zones along the tunnel. The first alternative is strictly based on the geological pre-investigations at site. The other one is more conservative, accounting for a potential larger number of deformation zones. To meet the aim, two research questions related to the case study application are to be answered:

1) Which of the alternatives is economically justifiable, according to the available data?
2) Is information from new core drilling investigations of value to the decision?

To reach the overall aim, specific objectives are:

- Development of a methodology of applying MPS algorithms in the SGeMS software for modelling of deformation zones in crystalline rock mass
- Development of a set of geological model realizations to quantify the geological uncertainty using the geostatistical simulation model SNESIM
- Quantification of the cost of making an erroneous interpretation of the number of permeable water-bearing deformation zones along the tunnel stretch
- Development of a methodology of quantifying the number of deformation zones encountered in a tunnel geometry in a modelled rock mass
- Development of a methodology for conducting a virtual sampling campaign for collection of additional data, consisting of several core drilling tests
- Development of a method for adjusting the expected amount of deformation zones encountered using a virtual core drilling campaign
- Quantification of the cost of collecting field data in the form of core drillings
- Evaluation of the potential economic value of performing further core drilling investigations (VOIA)

Given the broad scope and complex nature of the project, several limitations were introduced to adapt to the timeframe. The discussion segment of this report serves to present several points and topics where future research ought to be done to further develop the proposed framework.

- The study will be conducted on a case study of Kolmårdstunneln. Two grouting design options will be investigated, one being cheaper and sufficient for homogenous rock, the other one being more costly and sufficient for zones with high hydraulic conductivity, i.e. deformation zones. Furthermore, only two alternative grouting designs will be evaluated in the VOIA.

- The resolution of the grid used for the geological modelling will be relatively coarse for the purpose of efficiency, and since the additional deformation zones will be predicted on a large scale.
- The geological model will be defined binarily in the simulation algorithm used, including two different categories representing 1) “bulk rock” and 2) “deformation zones”. In all software, 0 will be used to represent bulk rock and 1 will be used to represent deformation zones.
- The geological model and the VOIA will only be performed for the purpose of addressing issues regarding tunnel grouting. As such, even though sampling might provide information valuable in other aspects, this will not be considered within the frame of this project. All comparisons done through CBA or VOIA are strictly economical. Hence, environmental impacts of sampling or insufficient grouting are not taken into consideration.
- Some of the associated costs will be determined through expert elicitation. Due to time constraints, these will be limited to a single expert elicitation per variable of interest.
- While the purpose of this project is to exemplify a methodology of providing decision-support using MPS and VOIA, the implementation of this decision-support in an actual project context will not be elaborated on.

2. Case study

An ongoing tunnelling project has been selected to enable exemplification of the multiple point statistics method and value information analysis. The tunnel chosen for the analysis is the project the Eastlink (Ostlänken) and more specific the tunnel Kolmårdstunneln. The project is part of an extensive railway development investment connecting several cities in south-eastern Sweden.

2.1. Study area

Kolmårdstunneln is located in south-eastern Sweden close to the city of Norrköping (Figure 1a). The area is characterized by a varying topography, ranging from <10 m near the shore and over 150 m further inland in the hilly areas (Trafikverket, 2021d). The net runoff in the catchment area is estimated to be 243 mm/yr (Trafikverket, 2021a). Within the area surrounding the tunnel, there are several lakes, watercourses, and wetlands, some of which have been determined to have high conservational value due to being unpolluted (Trafikverket, 2021a). Especially the lake Skiren has been determined to be of importance to preserve, as it is not only unpolluted, but also houses many rare species and supports the surrounding forest which is also rich in natural value (Trafikverket, 2024). Since the lake is sensitive, precautions must be taken in any project which could influence either the water levels or chemistry of it. The entirety of the study area is rural, and any damage caused by the project will hence be related to the formerly discussed natural objects and values. The extent of the tunnel is shown in Figure 1b.

Figure 1: a) The location of the study area, b) the location and extent of Kolmårdstunneln.

2.2. Geology of the study area

Description of the geology and its inherent characteristics in the frame of this project is based on the engineering geological prognosis conducted by Trafikverket (2021a). This prognosis is based on mapping done by the Swedish Geological Survey (SGU) in conjunction with investigations through terrain surveys, core drilling tests and pump tests conducted between years 2015 and 2018. Core drilling tests results and deformation zone interpretations based on maps from SGU have been used to characterize the fracture and deformation zone networks.

The bedrock of the study area is comprised almost entirely of crystalline bedrock related to the Sveconorwegian orogeny (Trafikverket, 2024). The rock is mostly granite based, and the local groundwater would hence be in the fracture network. A comprehensive map showing deformation zones in the area interpreted by SGU is presented in Figure 2. This map is based on geological field observations in combination with results from geophysical analyses and provides information regarding large scale trends in the fracture network in the rock mass.

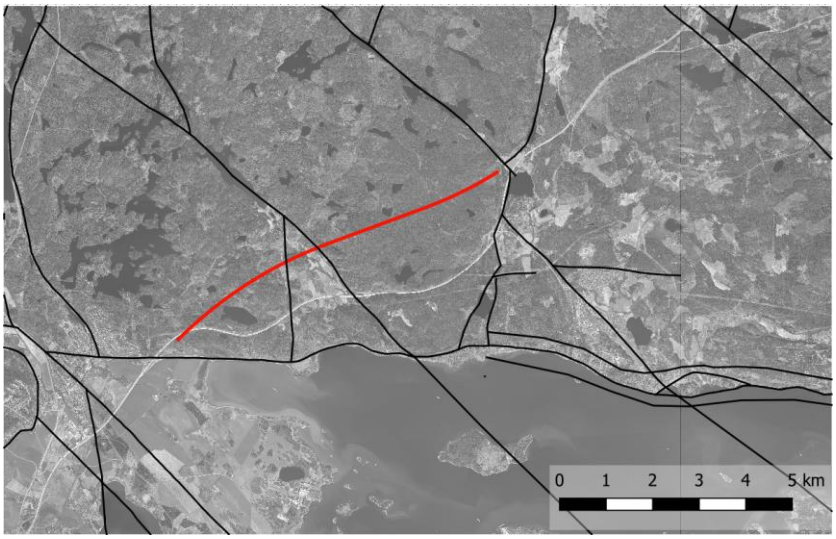

Figure 2: Interpreted deformation zones in the study area, the red line represents the tunnel geometry. © Sveriges geologiska undersökning. (2024).

Interpretations of additional field mapping along the tunnel, performed by SGU are illustrated in Figure 3 (Trafikverket, 2024).

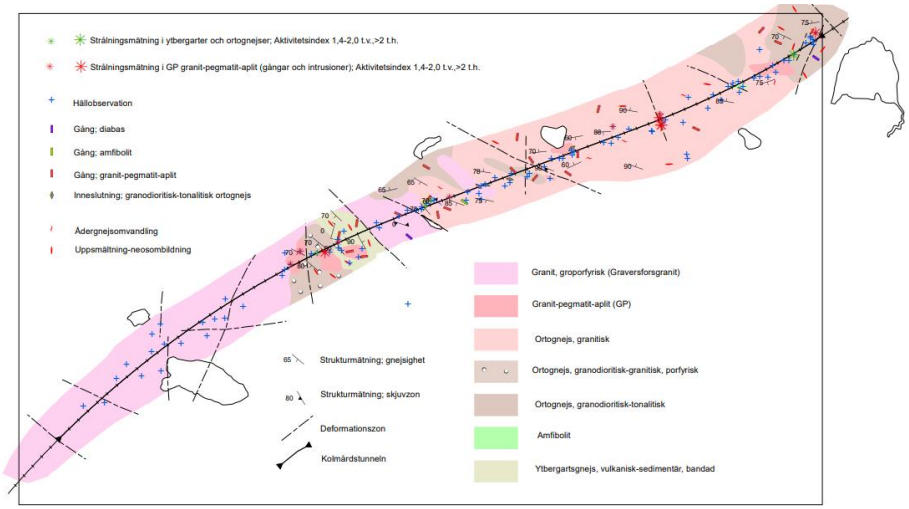

Figure 3: Interpreted deformation zones along the tunnel, mapped by SGU (Trafikverket, 2024).

Locations of the core drilling tests conducted between 2015 and 2018 are illustrated in Figure 4. Most of these have been performed in the southwest part of the tunnel area. Additional core drilling campaigns have been planned for conduction in the spring of 2024. Data that has been gathered through core drilling tests is used as conditioning data within this project. According to a geological survey of the area conducted by SGU, 17 weakness zones exist along the tunnel (Trafikverket, 2021a), 5 of which have been verified by core drilling investigations.

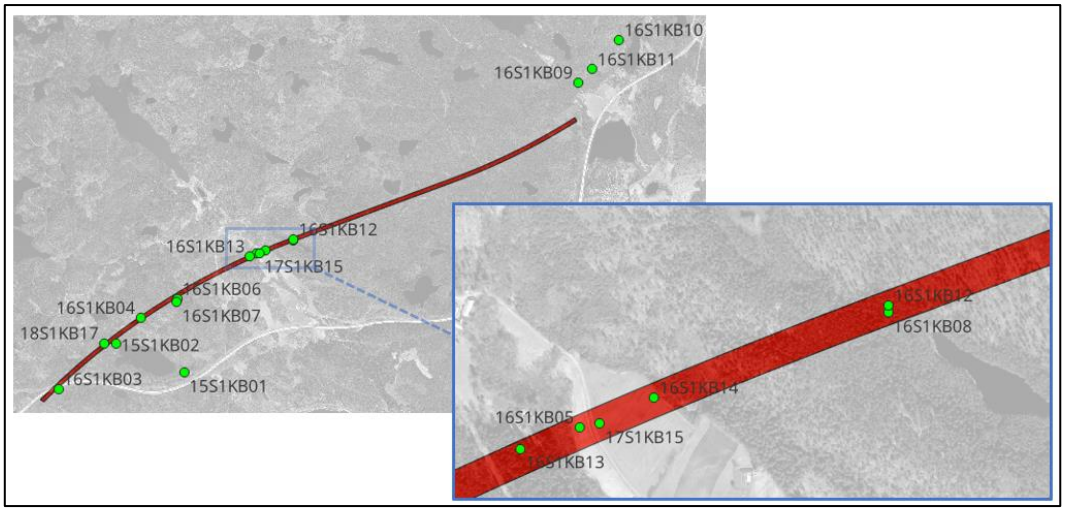

Figure 4: Locations of the performed core drilling tests. The red line represents the tunnel.

The tunnel stretches through three structural geological domains (Trafikverket, 2021a). The division into structure geological domains (SD1, SD2 and SD3) are of particular interest due to them being highly associated with deformation zone characteristics. The structure geological domain division has been made because of geographical variation in trends for crack related parameters such as strike and dip. A map over the tunnel, divided into the three structure geological domains are presented Figure 5. Of the 17 interpreted weakness zones along the tunnel, 6 are in SD 1, 4 in SD 2 and 7 in SD 3. Details regarding strikes and dips associated with the different structure geological domains are attached in Appendix 1 through Appendix 6.

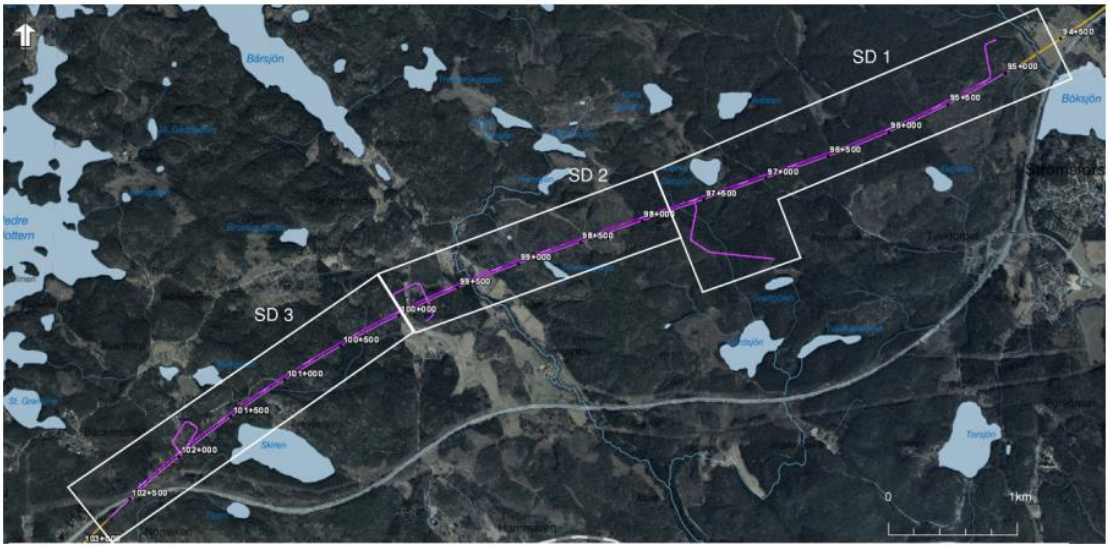

Figure 5: Map over the tunnel, divided into the three structure geological domains SD1, SD2, and SD3 (Trafikverket, 2021a).

2.3. Structure of the tunnel

The tunnel construction constitutes one railway tunnel and one service tunnel (Trafikverket, 2021d). The railway tunnel has an open cross-sectional area of 91 square meters to minimize the resulting increase in pressure that would come with trains passing through at high speed, while the service tunnel has an open cross-sectional area of 31 square meters to allow for emergency vehicles to easily pass through (Trafikverket, 2021d). The two sub-tunnels lie 15.5 meters separated from each

other, with connections and an increase in width every 400 meters to allow for grouping of emergency vehicles. At these sections of extended width, the distance between the tunnels is 10 meters. Figure 6 shows the profile and cross-sections of the two tunnels (Trafikverket, 2021d). The tunnel is planned to be constructed in the bedrock under an area dominated by woodland and small lakes, at a depth spanning between approximately 10 and 140 meters down in the bedrock. Both the south-western and the north-eastern entrances to the tunnel are located close to the highway E4. The profile of the tunnel, showing the topography above the tunnel is illustrated in Figure 7.

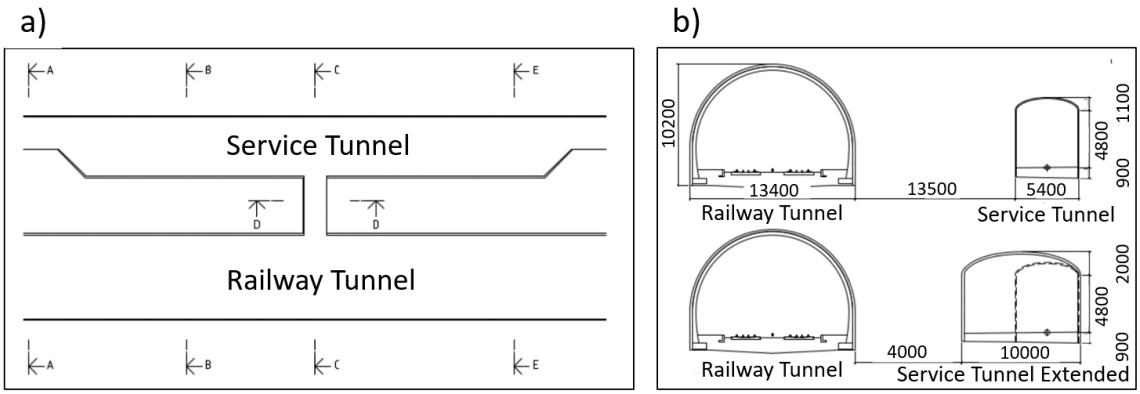

Figure 6: a) Profile of the railway tunnel and service tunnel. b) Cross-section of the railway tunnel and the service tunnel. Image from (Trafikverket, 2021d)

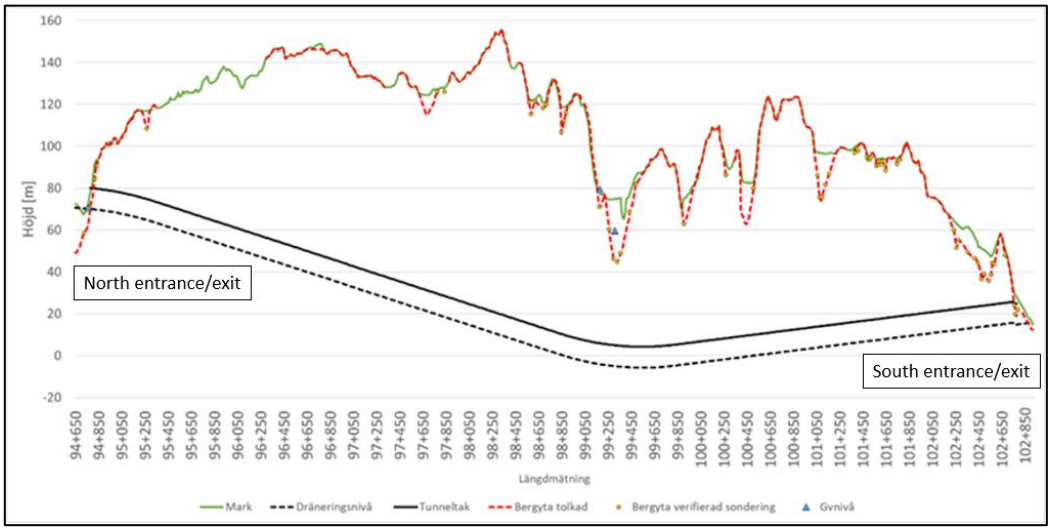

Figure 7: The profile of Kolmårdstunneln (Trafikverket, 2021c)

2.4. Grouting in the Kolsmårdtunneln project

When dealing with underground construction such as tunnelling, leakage of groundwater is an issue that must be considered (Grøv & Woldmo, 2012). One of the main objectives regarding groundwater leakage consideration in underground construction is to avoid water from entering the excavation, another is to protect the surrounding area from unwanted events caused by leakage induced groundwater drawdown. Regarding construction in rock mass, cracks and deformation zones are of major concern since the hydraulic conductivity and interconnectivity of these constitute pathways that may enables transportation of large amounts of water (Grøv & Woldmo, 2012). To avoid water

masses to leak into underground excavations via cracks and deformation zones, pre-grouting is a broadly used and effective measure. The technology implies that grouting material is injected into the rock mass, filling the cracks with a hardening material before excavation (Grøv & Woldmo, 2012). This creates a medium with lower hydraulic conductivity, hence reduces the amount of water leaking into the tunnel. Different grouting strategies, e.g., different grouting materials are selected depending on the permeability of the surrounding rock mass and the hydrological conditions at site (Grøv & Woldmo, 2012). Since different grouting strategies are associated with different economical costs, collection of hydrogeological data and knowledge regarding the hydrogeological conditions are of great importance. In Figure 8, a typical case of pre-grouting during a tunnel construction project is shown. The grouting fan has a control drilling angle of 7 degrees with a length of 18 meters, and an injection hole angle of 14 degrees with a length of 21 meters and overlap of 5 meters between injection holes.

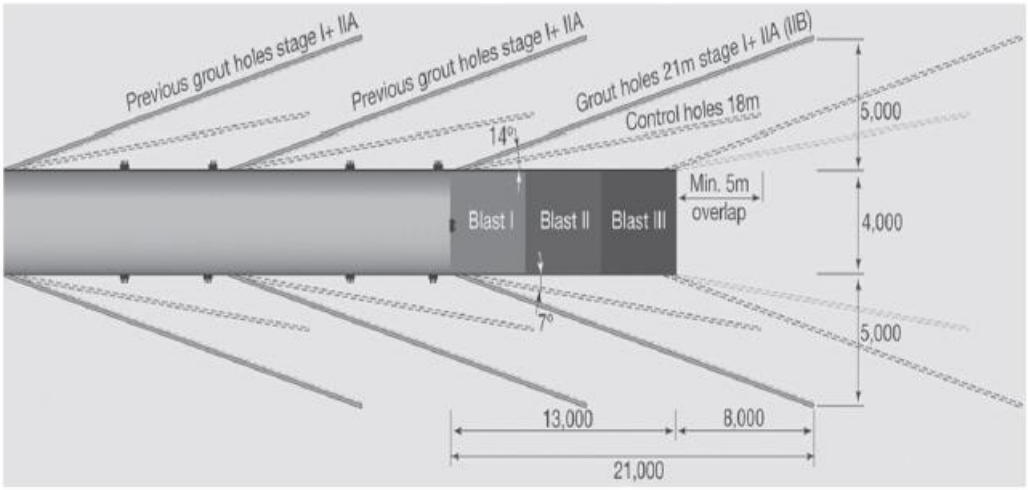

Figure 8: Example of a pre-grouting design (Grøv & Woldmo, 2012).

In the project of this case study, an early-stage injection concept has been designed (Sweco, 2021). According to the corresponding report, the tunnel is primarily excavated in what is expected to be rock with low permeability. At the time of conducting this project, final legal requirements set in the permit from the land- and environmental court were yet to be made regarding threshold requirements related to water leakage (Sweco, 2021). Hence, for the sake of designing an injection concept, pre-emptive requirements were set. A leakage threshold of 15 liters per minute per 100 meters of tunnel has been set for the majority of the tunnel, with a stricter requirement of 4 liters per minute per 100 meters of tunnel for the part of the tunnel close to lake Skiren, which is considered a sensitive area. To meet these different requirements, different grouting classes are used. While the low-requirement parts of the tunnel might only require a single injection of cement, more considerable measures with silica-based material for injection might be required for the parts with higher requirements (Sweco, 2021).

3. Method

The following subsections contain both brief introductions relating to the methods used, and explanations of the methods themselves. First, the general approach is presented in section 3.1, followed by detailed information of the methods used in section 3.2 and 3.3.

3.1. General approach

The methodology proposed in this project is comprised of two main parts; 1) construction of a geostatistical model, using a multiple point statistics algorithm, and 2) a value of information analysis (VOIA). For the construction of the geostatistical model, the Stanford Geostatistical Modelling Software (SGeMS) has been used for simulation. SGeMS is a tool comprised of several different geostatistical algorithms useful for describing space-time distributed phenomena in a user-friendly and easy to digest way (Remy et al., 2009).

A flow chart including key tasks for the project execution, divided into the two separate blocks "Geostatistical modelling" and "Value of information analysis" is presented in Figure 9. The tasks are ordered chronologically where all tasks within the "Geostatistical modelling" block are done before starting with the "Value of information analysis" block. Sources of information/data for certain steps are presented underneath the blocks in green boxes, and outputs/results from tasks are presented in red boxes. Following tasks constitute the method:

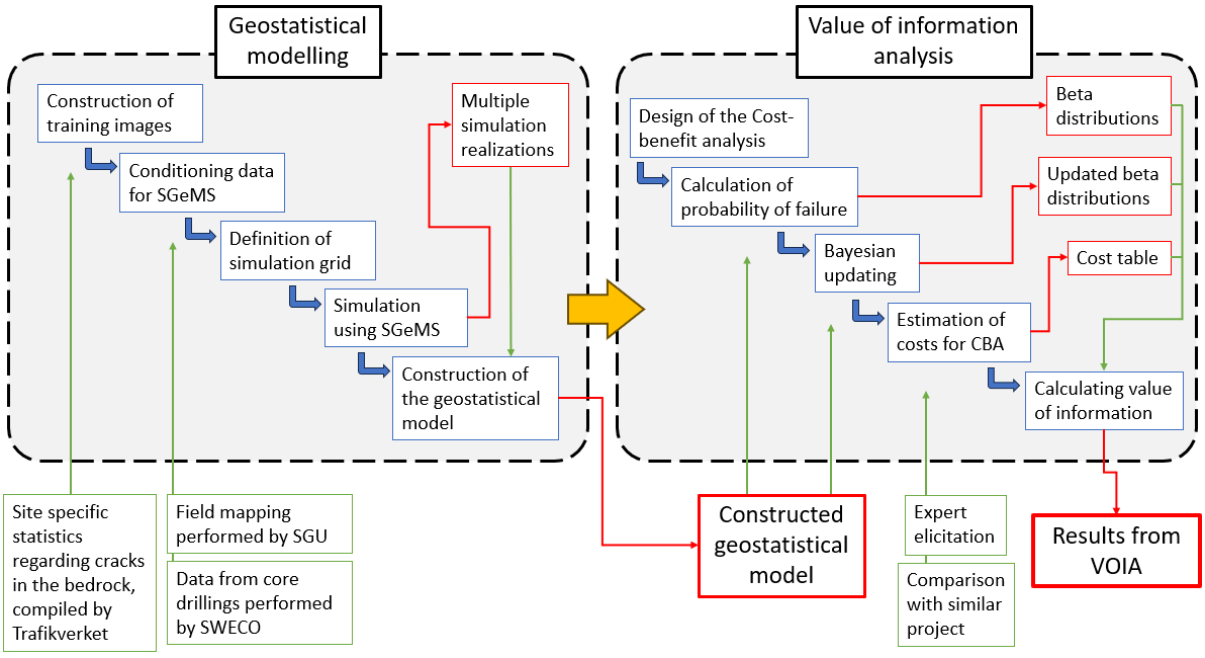

Figure 9: General approach of the project illustrated as a flow chart. Specific tasks are divided into two separate blocks: "Geostatistical modelling" and "Value of information analysis". Green arrows refer to inputs to certain tasks within the flow chart. Sources of information used for certain tasks are presented in green boxes below the flow chart. Red boxes refer to ouputs from tasks.

Listed below is a further clarification of the tasks:

- **Construction of training images:** 3-dimensional training images are constructed according to site specific statistics regarding cracks within the different structure geological domains (SD1, SD2, and SD3). Training images are then used for simulation in the SGeMS software.

- **Conditioning data for SGeMS:** Conditioning data, in terms of deformation zones interpreted from field mapping, and results from core drilling tests, is compiled and prepared for importation to SGeMS. During simulation, the conditioning data serves as conditioning data points, between which the simulation algorithm extrapolates additional deformation zones according to patterns in the training image.
- **Definition of the simulation grid:** A simulation grid consisting of a pre-defined number of cells in the x-, y-, and z-directions including the conditioning data as well as the tunnel geometry is created in the SGeMS software. Simulating on the grid will result in all cells being assigned information regarding either deformation- or non-deformation zone.
- **Simulation using SGeMS:** This step includes selection of several parameter values included in the MPS-algorithm used and performing an adequate number of simulation iterations.
- **Construction of the geostatistical model:** All simulation realizations are summarized for the purpose of constructing a probability-based model. The result of this is a grid where each of the related cells has a certain probability of deformation zone. This finalized geostatistical model is the base of all following work associated with the VOIA.
- **Design of the cost-benefit analysis:** To perform the cost-benefit analysis, a reference alternative grouting design (A1) and a secondary alternative (A2) for the tunnel was defined. The difference in the grouting design alternatives is in the number of expected deformation zones encountered along the tunnel, A1 expecting less and A2 expecting more. The implication of this is that A1 comes with a smaller construction cost, but with a potentially larger cost of failure. Likewise, A2 comes with a larger construction cost but with a smaller potential cost of failure.
- **Calculation of probability of failure:** This calculation is performed on the constructed geostatistical model, where all cells in the simulation grid intersecting with the tunnel geometry is isolated. A Monte-Carlo simulation is performed on the number of deformation zones encountered in the analysed cells. This allows for beta distributions for alternatives A1 and A2 to be established, describing the probability of exceeding their respective expected number of deformation zones.
- **Bayesian updating:** A virtual sampling campaign is designed and conducted. The additional information gathered in this virtual sampling campaign is used to update the already established beta distributions associated with the simulated outcomes of A1 and A2. Thereby moving from a prior to a pre-posterior probability.
- **Estimation of costs for CBA:** Costs associated with 1) tunnel construction, 2) underestimating the number of deformation zones, and 3) conduction of core drilling tests are estimated. This is done through expert elicitation and comparison with a similar tunnelling project.
- **Calculating value of information:** Cost-benefit analyses are performed for alternatives A1 and A2 both before the Bayesian updating (prior analysis) and after (pre-posterior analysis). The value of information gathered through the virtual sampling campaign is then calculated by comparing the prior analysis cost with the pre-posterior analysis cost. The campaign is seen as worthwhile if it results in a different alternative being cheaper in the pre-posterior analysis as compared to the prior analysis, and the value of information exceeds the cost of conducting the campaign.

All specific tasks included in the flow chart are described in detail under following subsections 3.2 and 3.3.

3.2. Geostatistical modelling with multiple point statistics

This section covers the methods used within the geostatistical modelling block. Since these require some basic knowledge regarding geostatistical modelling and multiple point statistics, an introduction to the topic is given in section 3.2.1. Then, the following subsections aim to describe the methods related to all tasks included in the geostatistical modelling block.

3.2.1. Theory and basic concepts

When constructing a geostatistical model, the available data is oftentimes sparse due to the costs and difficulties of sampling (Davis et al., 2002). Many different methods of spatial interpolation exist, with differing advantages and disadvantages in terms of especially quality and complexity. As such, choosing an appropriate method for constructing an interpolated model space is of high importance when conducting geostatistical analysis in general (Tahmasebi, 2018).

Perhaps the most commonly used and well-established method of spatial interpolation in geostatistics is the Kriging method (Davis et al., 2002). Kriging is a two-point method of interpolation, making use of the variance between data points to help fit a theoretical variogram to the discrete data pairs in order to construct a curve capable of describing continuous variability in space for a given distance (Davis et al., 2002). This method is computationally efficient and has the added advantage of taking clustering into account by evaluating each data point based on proximity to the others. However, despite its wide usage, the Kriging method has a number of weaknesses that makes it unfit for the purposes of this project. Primarily, any two-point method will run into the issue of struggling to handle more complex and heterogeneous spatial structures and patterns, as handling two points of information at a time does not provide sufficient context (S. Strebelle, 2002). The issue of only using two points at a time can be seen in any given theoretical variogram used for the purposes of Kriging, as the continuous curve will almost always overestimate lower values of variance, while underestimating higher values, leading to excessive smoothing (Tahmasebi, 2018). To overcome the aforementioned issues of failing to represent uncertainty and the more complex patterns and structures that emerge in deformation zones and fracture networks, multiple point statistics could be a suitable alternative as a method for spatial interpolation (X. Liu et al., 2009).

Multiple point statistics (MPS) aims to move away from the limitations set by relying on covariance between data pairs as a means of interpolation, instead it opts to use a so-called training image (TI) which is a conceptual image representing possible patterns that may occur together with conditioning data points to construct a model space (Strebelle & Journel, 2001). A simplified way of looking at this process is that the TI is decomposed into a library of possible patterns, that are then fit together in accordance with the conditioning data.

The SNESIM algorithm works by scanning the training image for replicates of the conditioning data and building a sub training population of which conditional distributions can be defined, whereafter the model is built pixel by pixel sequentially (Tahmasebi, 2018). Initially the algorithm was structured as an extension of indicator Kriging (Guardiano & Srivastava, 1993). The current-day SNESIM algorithm has been updated to make it more efficient through the added construction of a search tree during the simulation, which means that the training image only has to be scanned once during the process (S. Strebelle, 2002). The algorithm is however practically limited to simulation of data sets with fewer categories (less than four, with no continuous variables) and it is also demanding of a rich in data training image, that can fulfill the criteria of providing multiple replicates of occurring structures in the conditioning data (Remy et al., 2009). The algorithm can make use of either a single grid or a multiple grid approach where for the former, a random path is used to fill in the entirety of

the simulation grid and for the latter, the model structure as a whole is divided into different levels of coarseness, each with its own search tree. The multiple grid method is better suited for large scale structures (Remy et al., 2009).

3.2.2. Construction of training images

The training image is the input data that aims to represent all the different patterns and structures emergent in the to-be model (Strebelle & Journel, 2001). It can be constructed in a number of ways, including object-based methods where the geometries are built with algorithms, process-based methods where 3D-models are built by simulating natural processes and outcropping where simple images are used to create the TI. The latter of which can be particularly useful for representing unique patterns and structures that are often seen in geology in for example fracture or deformation zone networks (Tahmasebi, 2018). Once a training image has been established, it can be scanned, discretised, and decomposed into a pattern library which can be used to build the different structures and patterns apparent in the TI. It is important to note that the TI does not contain any concrete spatial information in terms of coordinates or scale but is only useful in providing the model with guidelines for how the patterns and structures emerge within it based on attributed raw data (in this context called the conditioning data) (Tahmasebi, 2018). If different patterns exist in distinct areas of the model, thus if there are non-stationary conditions, the model space can be subdivided into regions that each can make use of their own TI (Remy et al., 2009).

Training images were constructed based on statistics regarding fractures in the bedrock (strike, dip, and intensity) along the tunnel. The compilation of these statistics was performed within the frame of the Kålmordstunneln project, for the purpose of the tunnel design support (Trafikverket, 2021a). During training image construction, matrixes including the statistics regarding crack strike and dip were manually created. Information regarding the different structure geological domains was used to create three hypothetical training images. The training images were constructed to match the fracture characteristics associated with the different domains. This was done since the characteristics of fractures were assumed to be representable for deformation zones. Details regarding 1) strikes, 2) dips, and 3) quantities of cracks, used for training image construction are presented in Table 1. This selection was based on interpretations of information attached in Appendix 1 through Appendix 6.

Table 1: Selected strikes, dips and quantities of cracks used to create training images corresponding to the different structural geological domains.

Domain	Crack group	Strike°	Dip°	Cracks (quantity)
SD 1	**SG-1**	255	85	2
	SG-2	310	80	2
	SG-3	15	60	1
SD 2	**SG-1**	140	75	3
	SG-2	235	65	2
	SG-3	240	30	2
SD 3	**SG-1**	90	60	2
	SG-2	280	65	2
	SG-3	230	80	4

Figure 10 shows an example of training image construction. Three matrixes containing information of: 1) crack/non-cracks, 2) associated strikes and 3) associated dips for each of the three structure

geological domains were defined in 2D matrices for later conversion to 3D using scripts. The 2D-training images representing structure geological domains 1 through 3, before being converted to 3D are presented in Figure 11.

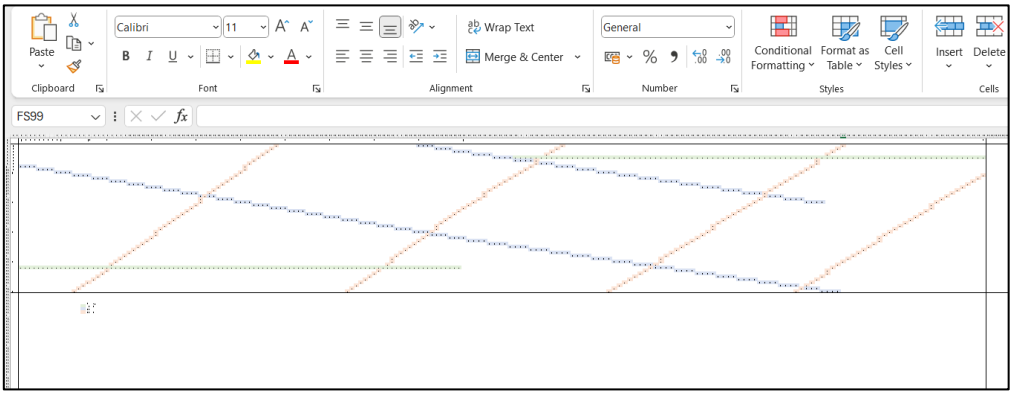

Figure 10: Example of a grid (structure geological domain 3) including cracks created in Excel (200 X 50 cells). The different colours correspond to different strikes and associated dips.

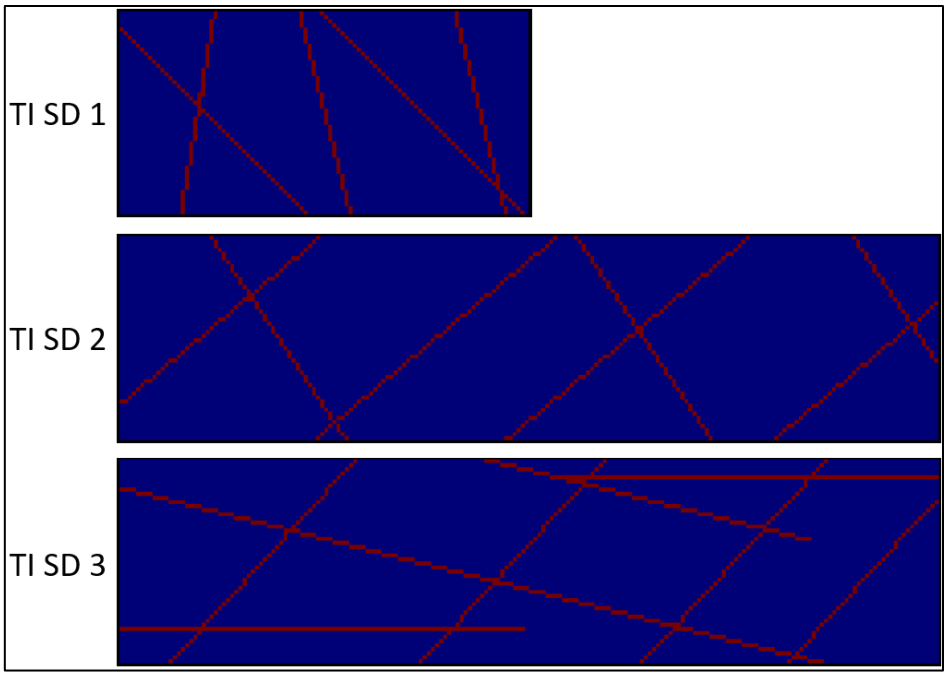

Figure 11: Two-dimensional training images representing structure geological domains 1 through 3.

Once the 2D training images had been created, a script was developed to generate new ones in 3D for usage in SGeMS using the information regarding strike and dip. The script has the following procedure, with a visual example showcased in Figure 12:

1. A 2D-training image is defined as a matrix with an indicator 0 for bulk rock and an indicator 1 for deformation zone. Each of these matrices also has corresponding matrices featuring strike and dip values for every element with a deformation zone.
2. The elements in the 2D-training image matrix are checked one by one. If an element featuring the indicator 1 is encountered, a 3D-matrix is constructed by extrapolating the deformation zone to a target depth using the corresponding strike and dip values.

3. Once a 3D-matrix has been built, the script moves on to the next element featuring an indicator 1 and repeats the process, continually adding new 3D matrices to each other, superpositioning them.
4. Once all cells all of the 2D-training image matrix have been checked, cells with values above 1 are set to 1 to account for overlap and the end product of a 3D-training image has been constructed.

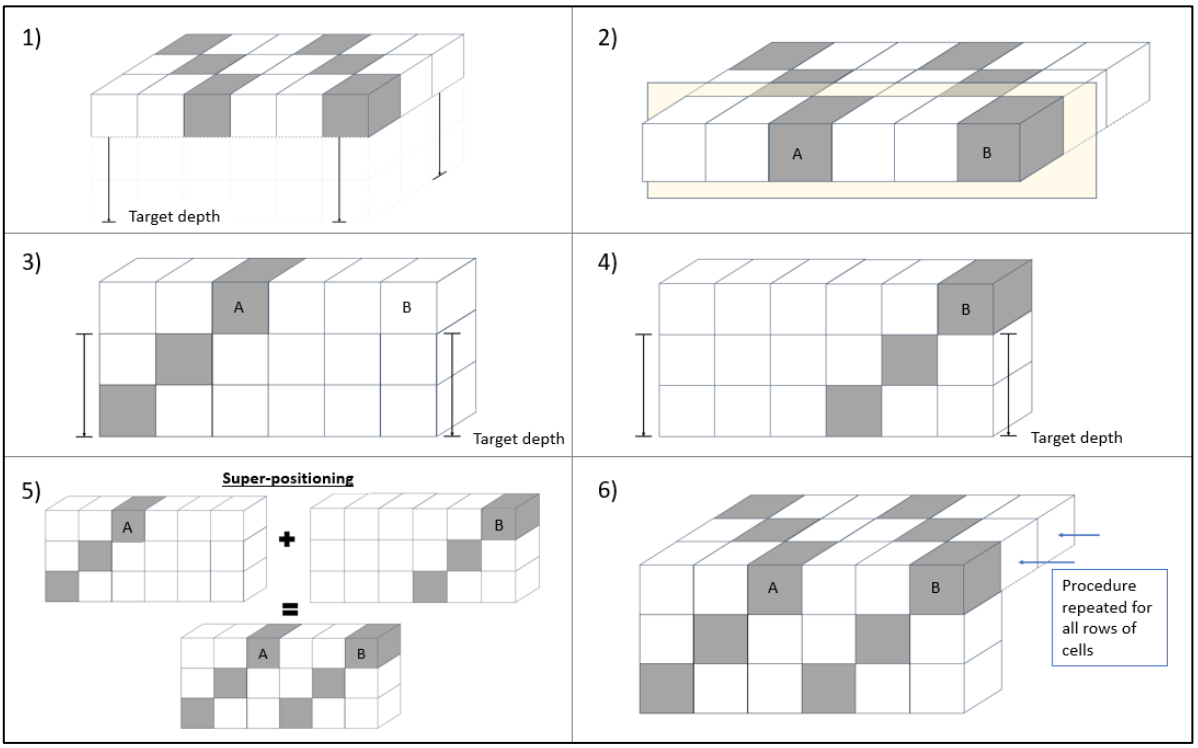

Figure 12: Illustration of the MATLAB script creating a 3-dimensional grid from a 2-dimensional training image, with associated strikes and dips. Strike is 315° and dip is 45° in this example. Deformation cells are grey.

The constructed Training images associated with the different structural geological domains are presented in Figure 13.

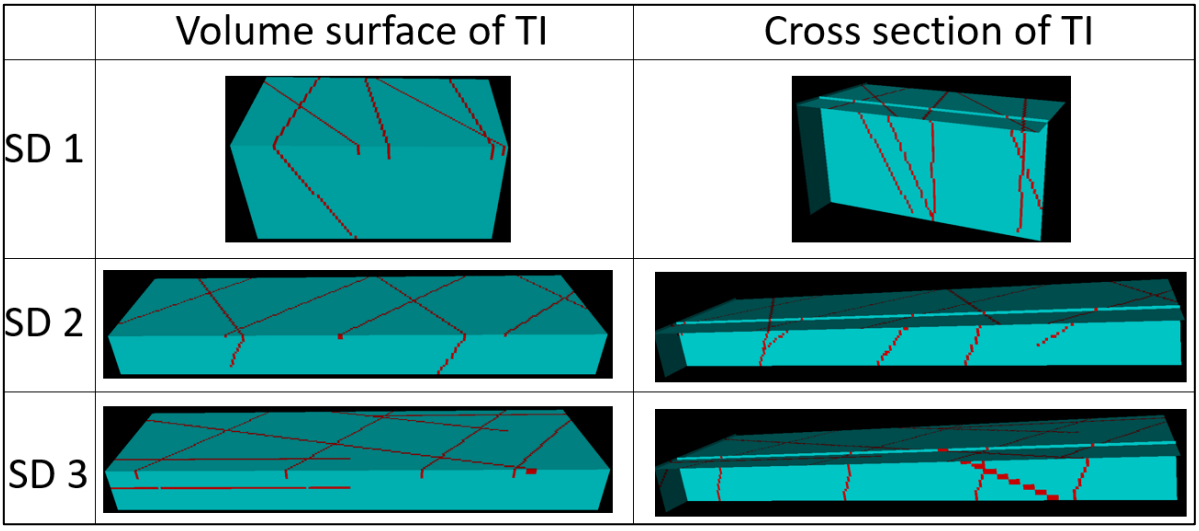

Figure 13: Constructed training images regarding structural geological domains 1 through 3. Cross sections are presented to illustrate the dips inside the volumes.

3.2.3. Conditioning data for SGeMS

The second type of input necessary for MPS is the conditioning data, which is the raw, discrete data used for the actual interpolation when constructing the model (Strebelle & Journel, 2001). A distinct advantage of MPS in comparison to variogram-based methods is that an accurate model can be built even with a small amount of datapoints, as long as the expected patterns and spatial structure can be described by the training image (Tahmasebi, 2018).

The core drillings presented in Trafikverket (2021b), where converted into vectors with a binary indicator representing deformation zone or no deformation zone, these vectors were used as conditioning data for the SNESIM simulation. Additionally, deformation zones along the tunnel interpreted by SGU was also used as hard data at the ground level.

3.2.3.1. Conditioning data treatment

The data obtained through core drilling tests was manually imported to a GIS software. Information regarding core drilling direction, angle, sample length, elevation, and occurrence of deformations/cracks along the core drilling samples were used to calculate positions of deformations/cracks. To import this data in SGeMS, some treatment of it was needed. The core drilling test information contained data regarding 1) core drilling starting coordinates, 2) core drilling end coordinates and 3) coordinates for encountered deformation zones. The larger part of each core drilling test constitutes of rock mass. To interpolate residual points with no deformation a script was built.

The script creates a chosen number of points, at an even interval, between the starting coordinate and the end coordinate of each core drilling test. If any deformation zones exist in the core, values of one are assigned to the closest generated point. Depending on the chosen number of points created, there may be cells in the simulation grid containing several interpolated points. This may have problematic implications due to the way SGeMS handles such situations. If a zero and a non-zero value would appear in the same grid cell in SGeMS, the program would automatically assign a zero value to the cell and the deformation data would thereby be lost. To avoid this, a boundary value was defined such that any non-deformation points appearing within a particular range of a deformation zone point would be assigned “NaN”. The procedure of this operation is illustrated in Figure 14. In SGeMS, the core drilling data will take on the appearance of long rows of points featuring values of zero, with isolated points featuring values of one (exemplified in Figure 15).

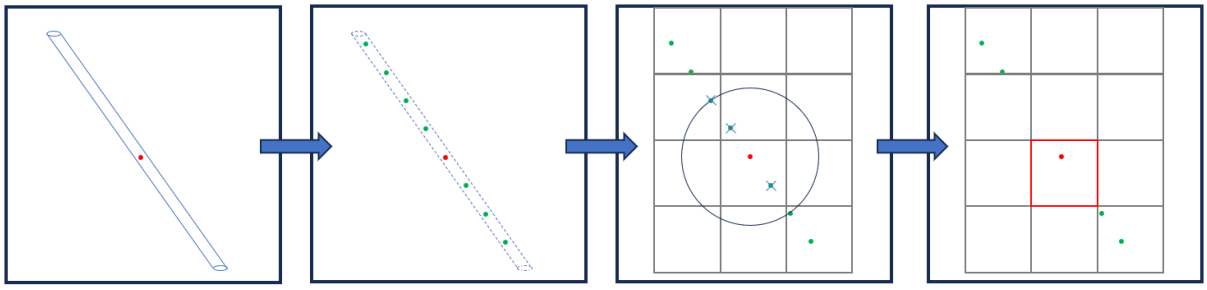

Figure 14: Procedure to remove non-deformation core drilling data points close to the deformation core drilling data points. The red dot represents a deformation data point (value=1) occurring in a core drilling test, green dots represent interpolated non-deformation data points (values=0) with regular intervals.

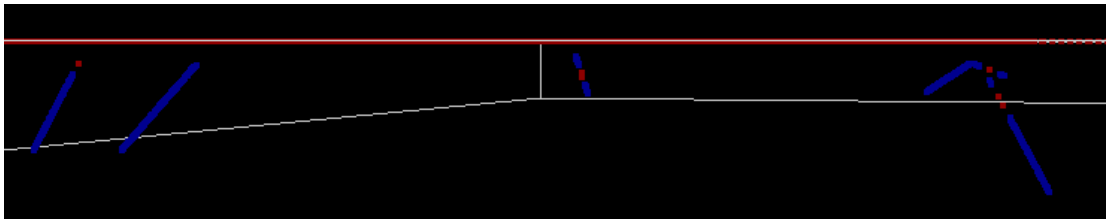

Figure 15: Several examples of core drilling test results defined in SGeMS. Blue dots refer to non-deformation points, red dots refer to deformation points.

The positions and extents of the deformation zones interpreted by SGU were manually drawn and used as conditioning data. Since the dips associated with these deformation zones are only based on expert judgement, they have not been used as conditioning data. Instead, only the deformation zone positions on the ground level have been included as hard data. The deformation zones mapped by SGU appeared to have strikes that differed from the ones defined in the training images. As a result of this, simulation results showed a lot of seemingly random results caused by extrapolation with unmatching strike (as defined in the training images) from mapped deformation zones. To reduce this effect, additional deformation zones with strikes matching the mapped deformation zones were added in the training images (exemplified in Figure 16). These strikes have been matched with dips presented in Table 1.

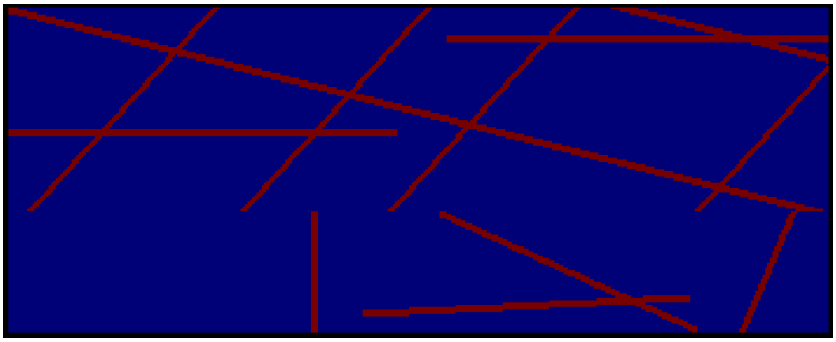

Figure 16: Training image regarding SD3, complemented with strikes mapped by SGU.

3.2.4. Definition of simulation grid

To enable simulation in SGeMS, a simulation grid must be defined, and in the specific case where three different training images were to be used for the different structural domains, the simulation grid had to be divided into three regions corresponding to the different domains, as illustrated in Figure 17. Cell sizes of 10 meters in the x-, y- and z-directions were selected. The size of the simulation grid was selected so that the whole tunnel as well as all the sampled core drilling data was captured within it. The depth of the simulation grid was set to 200 meters (20 cells).

For all following parts, only the region corresponding to SD3 have been modelled and analysed due to time constraints. Hence, the only training image used for the geostatistical modelling is the one based on statistics regarding cracks along the tunnel segment in SD3, complemented with strikes in the hard data mapped by SGU (illustrated in Figure 16). The regions corresponding to SD1 and SD2 have been included in the report for the purpose of exemplification and emphasizing differences between domains. Since SD1 and SD2 are not fully modelled, training images regarding these have not been used for anything other than trial simulations.

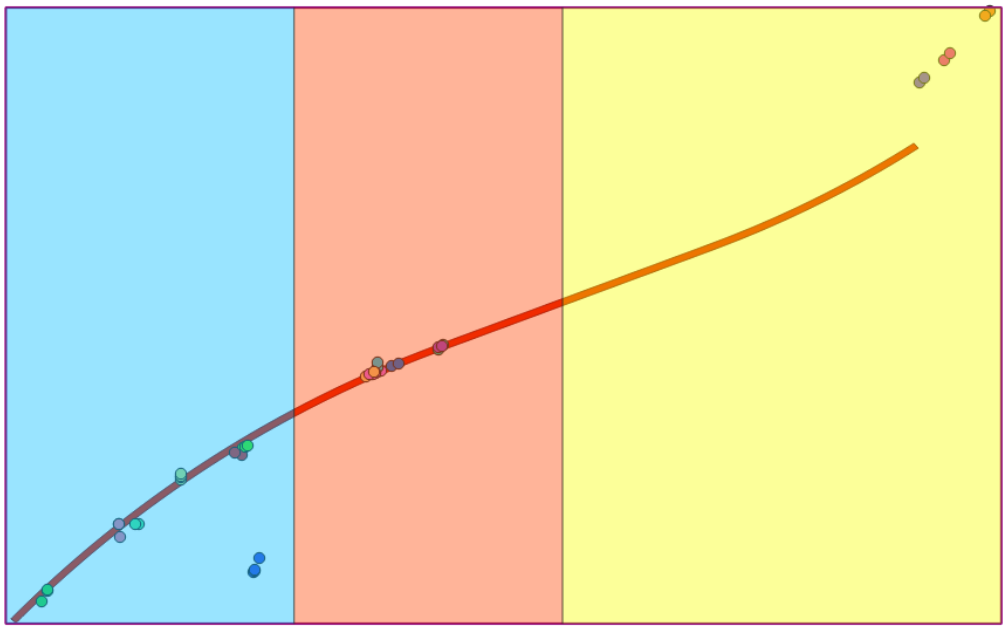

Figure 17: Division of the regions associated with structural geological domains done using QGIS. The yellow rectangle corresponds to SD1, the red to SD2, and the blue to SD3. The red line corresponds to the tunnel and the points correspond to sampled and calculated data points.

An illustration of the tunnel was imported to SGeMS. This was done both for the purpose of visualisation, and for further analyses associated with the VOIA. Since the simulation grid is defined as a rectangular block, some adjustment of the tunnel depth in relation to the ground level was needed. This was done by calculating and using the vertical distance from the tunnel to the ground level (ΔZ) as the tunnel depth defined in SGeMS and all further analytical work. An illustration of the tunnel level adjustment is presented in Figure 18, and the tunnel definition in SGeMS is presented in Figure 19.

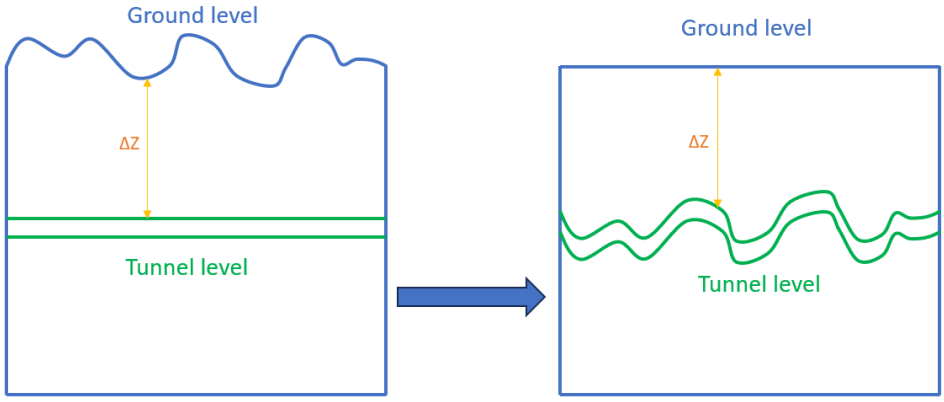

Figure 18: Adjustment of tunnel depth to account for the rectangular block shape of the simulation grid.

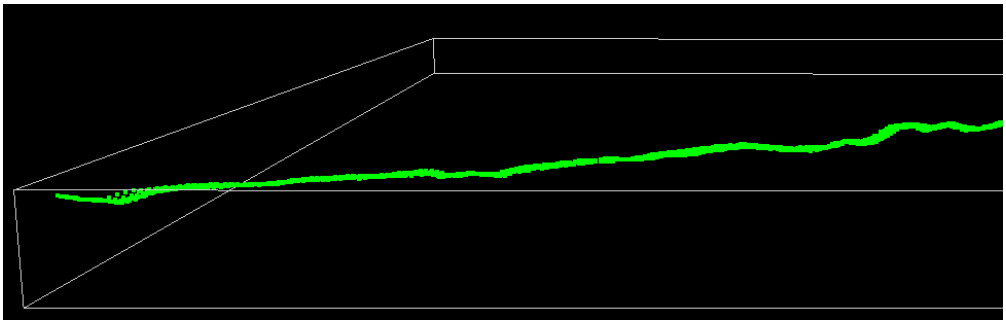

Figure 19: Definition of Kolmårdstunneln in SGeMS.

3.2.5. Simulation using SGeMS

The SGeMS user interface for the SNESIM-algorithm features a number of different settings and parameters to be set before the algorithm can be run. Figure 20 showcases the settings interface for SNESIM in the SGeMS software. Only the "General" and the "Advanced" settings are shown here as they feature the parameter settings of interest in the context of this project.

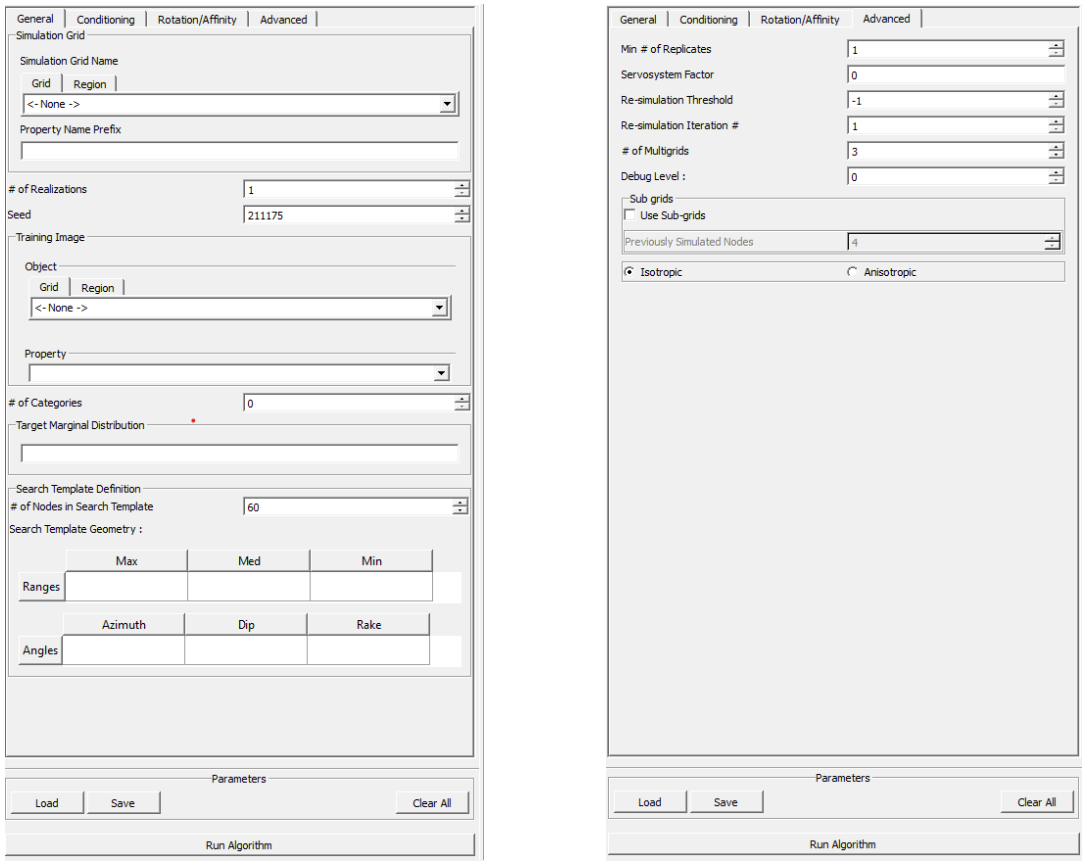

Figure 20: Setting interface of the SNESIM algorithm in SGeMS.

Input into SNESIM consists of a training image, conditioning data, and a simulation grid (Remy et al., 2009). In the "General" settings interface, the user can decide on number of iterations, the seed used for stochastic operations, what categories to simulate for, the target distributions of said categories for the simulation grid, the number of nodes used per element when generating the search tree and the geometry of the search template ellipsoid (Remy et al., 2009). Parameters of interest in the "Advanced" settings include:

- Minimum number of replicates- which refers to the minimum number of times a pattern has to show up in the training image in order to be taken into account.
- Servosystem factor- which for increasing values towards 1 will steer the generated model grid closer towards the target distribution set in the general settings.
- Number of multigrids- where multigrids refers to the approach of splitting up the grid into "rougher" and "finer" grids to better capture larger patterns.
- Subgrids- which help alleviate the data loss that occurs when sufficient replicates of a given pattern cannot be found (Remy et al., 2009).

According to Liu (2006), some general guidelines for these settings are:

- The target distribution of the simulation should not be too different from the training image.
- A high servosystem factor should not be used when constructing large-scale structures.
- Minimum number of replicates is not very sensitive unless performing servosystem correction but should be kept between 10-20.
- Multigrids should always be used and adapted based on the size of the largest structure relative to the size of the simulation grid.
- The search neighbourhood should be adopted to the structures that are to be reproduced but an isotropic ellipsoid is generally a good option and if using multiple training images, they should be consistent.

Furthermore, according to the user manual for SGeMS, subgrids are highly recommended to use in case of 3D modelling (Remy et al., 2009).

With the training images, conditioning data and simulation grid prepared, the SNESIM algorithm could be run in the SGeMS software. The settings used for running the SNESIM algorithm are listed in Table 2. All settings left unlisted had their default values used. These settings generally followed the recommendations from Liu (2006) with a low servosystem factor and a high number of multigrids, however, the search template geometry was kept isotropic as this showed the best generation of longer deformation patterns. Subgrids were used as this was strongly recommended for 3D simulations and re-simulation was not used since that resulted in a big increase in run time with no apparent improvement to the reconstruction of patterns.

Table 2: Settings used for SNESIM algorithm in SGeMS

Setting	**Value**
#of iterations	10
Target Marginal Distribution	0.95 ; 0.05 [no deformation ; deformation]
Number of nodes	200
Search template geometry	2000 ; 2000 ; 200 [max ; med ; min]
Minimum Number of Replicates	15
Servosystem factor	0
Number of multigrids	10
Subgrids	yes
Previously simulated nodes (subgrids)	10
Isotropic/Anisotropic	Isotropic

The algorithm output showed high sensitivity towards changes in many of the parameters, definition of the search grid, size of the training images and resolution of the grid. In many cases, modifying the settings to achieve better pattern reconstruction resulted in a drastically increased run-time for

the algorithm. Because of this, a general strategy used was to run the algorithm with a smaller search grid while examining the setting parameters. This was done until the settings achieved sufficient complexity in terms of reconstruction of patterns on the simulation grid. Once an adequate set of parameters and settings was established, these were used for running the total number of iterations with a more detailed search grid to improve results.

Trial simulations performed with different test training images indicated that the SNESIM algorithm could better reconstruct and extrapolate continuous lines if they were defined with a width larger than one cell in the training image selected. For this reason, all training images used, as well as the conditioning deformation zones at the surface mapped by SGU, was defined with a width of 3 cells. As a result of this, the deformation zones reconstructed in the simulations would also have a width matching the ones in the training images, i.e. 3 cells.

3.2.6. Construction of the geostatistical model

Running the SNESIM algorithm in SGeMS with settings presented in section 3.2.5 and the conditioning data described in section 3.2.3 results in 3-dimensional grids constituting of cells representing either solid rock mass or deformation zones. Three examples of simulation realizations are presented in Figure 21. There are both some differences and some similarities between the three realization examples presented. However, the relatively high level of randomness in the simulations is problematic in further analyses due to it creating clusters of deformation zones with high geometrical variety among the realizations. This results in large proportions of deformation zones with a lot of uncertainty. To handle this issue, a probability-based model approach was used, considering the randomness and uncertainty of the individual simulation realizations. The probability-based model would hence represent the similarities between the realizations, in terms of repeatedly simulated deformation zones.

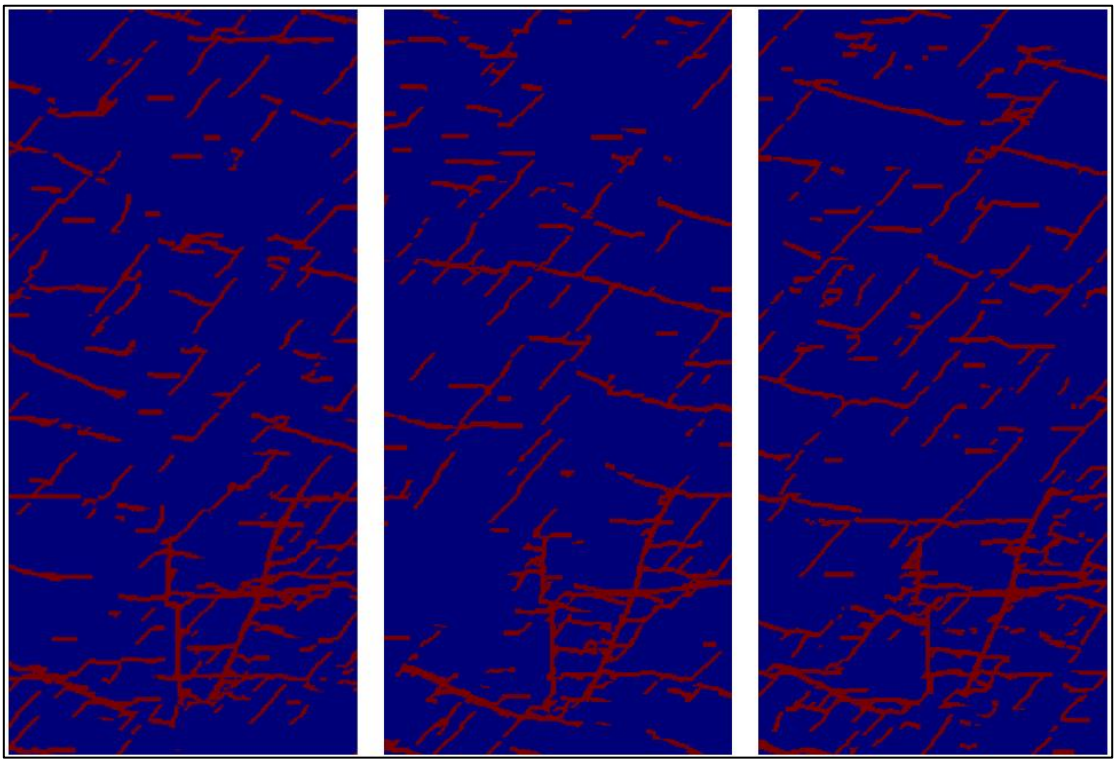

Figure 21: Three different simulation realization examples.

To create a model containing information regarding probabilities of deformation zones along the tunnel, a total of 200 simulation iterations were performed. The results of these simulations were then summarized and divided by the number of iterations performed, resulting in probability-based model containing probabilities ranging from 0 to 1 for each cell (illustrated in Figure 22). Cells that were simulated as a deformation zone in several of the realizations would thereby result in a higher probability of deformation zone in the updated model, than a cell that was simulated as a deformation zone in only one realization for instance. Another result of this is that cells containing conditioning data regarding presence of deformation zones is going to result in a probability of 1 (100%) in the updated model. As seen in Figure 22, this method results in a lot of noise in the areas where the conditioning data do not have any distinct influence on the probability of deformation zone. In the context of this project, these seemingly random deformation zone cells that are disconnected from the larger networks and trends and are unrelated to the hard data are viewed as noise.

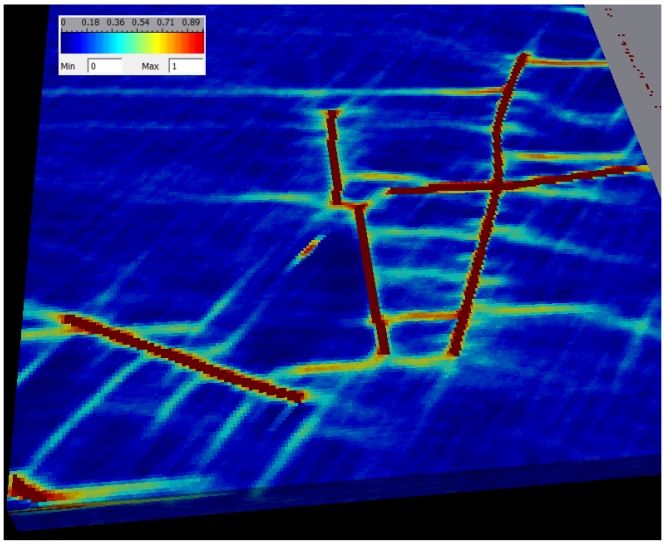

Figure 22: Illustration of the geostatistical model created in SGeMS using 200 realizations on structure geological domain 3. The grey area in the upper right corner is part of structure geological domain 2, hence is not included in this simulation and therefore contains no data.

3.3. Value of information analysis

The next step after establishing the geostatistical model was to use this very model to conduct value of information analysis (VOIA). To conduct the VOIA, several steps were taken. First, a Cost-Benefit analysis framework was designed to represent the reference alternative and the optional alternative given a set of construction costs, failure costs and probabilities extracted from the geostatistical model. After this, a virtual core drilling investigation campaign was designed to survey additional input that was used for the Bayesian updating step. The actual value of information is defined as the difference in value between the best performing alternative before the campaign and after the campaign- given that the better performing alternative changes after the fact (Freeze et al., 1992).

3.3.1. Theory and basic concepts

The following subsections serve to provide background context as to the function of Bayesian statistics and Value of Information Analysis in the project.

3.3.1.1. Bayesian statistics

The concept of a prior and a posterior probability serves as the basis in Value of information analysis (VOIA) where the value of collecting additional information is evaluated through Bayesian updating of a prior probability in the context of Cost-benefit analysis (CBA) (Freeze et al., 1992). Bayesian statistics differ from more conventional frequentist statistical analysis in that instead of viewing probability as the fraction of a certain outcome of an event given repeated trials, an initial probability is updated based on new information through a procedure called Bayesian updating (Clyde et al., 2022).

Bayesian updating makes use of Bayes rule as seen in equation 1 in order to adjust the prior, which is an initial probability of an event P(A) taking place, given the occurrence of another event P(B), in order to specify the posterior, which is the probability of the event taken place given that the other has already done so P(A|B) (Clyde et al., 2022). A basic example would be to consider the case of an unfair coin coming up as heads in a coin flip. The coin would initially be assumed fair, hence P(A)=0.5, but after collecting data through a number of flips, the initial assumption can be readjusted to take into consideration the additional data and a conditional probability of P(A|B) can be calculated (Clyde et al., 2022). In the context of Bayesian updating, P(B|A) as seen in equation 1 is called the likelihood and describes the probability of seeing the result B given assuming the prior probability is true. Furthermore, the procedure of Bayesian updating can be used iteratively, re-adjusting the prior and the likelihood given further collection of information.

$$P(A|B) = \frac{P(B|A) * P(A)}{P(B)} \tag{1}$$

The term in the denominator, P(B), is defined as presented in equation 2 and equation 3. Considering the definition of P(B), equation 1 can be rewritten as equation 4 which will be useful for the purposes of further analysis.

$$P(B) = \sum_{a \in A} P(B \cap A) \tag{2}$$

$$P(B) = \sum_{a \in A} P(B \cap A) = \sum_{a \in A} P(B|A)P(A) \tag{3}$$

$$P(A|B) = \frac{P(B|A)P(A)}{\sum_{a \in A} P(B|A)P(A)} \tag{4}$$

3.3.1.2. Value Of Information Analysis

In the early stages of a tunnelling project, uncertainty is a prevalent topic of interest (Freeze et al., 1992). Theoretical models regarding fracture zones and networks need to be verified by sampling in order to inform decisions regarding grouting methods, but these pre-investigations are often costly to perform and need to be balanced with the value gained by doing them- since an investigation which benefits do not outweigh its costs is better off not being done in the first place (Freeze et al.,

1992). A useful methodology for determining if and to what extent further investigations can be of value in the context of this kind of project is Value of information analysis (VOIA).

Within the field of decision analysis, VOIA comprises a method different from the normal expected utility-based decision analysis by putting further emphasis on the reduction of uncertainty within decision making (Keisler et al., 2014). "Value of information" describes the expected value of a decision with an added source of information relative to the value of a decision made without any additional information, as such it puts into context if the investigation required to receive this information is worth doing, based on the difference between the value of information and the cost of investigation (Freeze et al., 1992).

VOIA is generally performed in two steps; prior analysis and pre-posterior analysis (Freeze et al., 1992). In comparison to the typical posterior used in Bayesian statistics, the pre-posterior refers to the evaluation of alternatives after deciding on how new data should be collected- in regards to location and number of data points- but before doing so. Naturally, the pre-posterior analysis does not provide real measured values since no measurements have taken place, but the value of performing these investigations can be evaluated.

In the context of this project, where the value of information analysis is to be performed based on a tunnel in a geostatistically modelled rock-mass. The prior analysis can be done directly based on the geometry of the tunnel, whereas the pre-posterior analysis can be done based on virtual investigations done in the very same model- to see if the additional information collected would result in a different decision being made. The basic framework for analysis used here is called Cost-benefit analysis, which in its essence is a tool useful for economically comparing two alternatives based on their benefits, costs, and inherent risk costs (Johansson & Kriström, 2015). The concept of risk cost in this context refers to the economic cost of a specific consequence taking place and is associated with the probability of this specific consequence taking place. The sum of these benefits, costs and risk costs makes up the total value of a certain decision and is expressed as an objective function (Freeze et al., 1992). By comparing the values of different decisions, the most economically beneficial one can be determined.

3.3.2. Design of the Cost-benefit analysis

A cost-benefit analysis framework was designed to compare the value of the reference alternative and the secondary alternative, hereafter called A1 and A2. These two alternatives are separated by degree of preparation for expected deformation zones encountered during tunnel construction. Alternative A1 refers to a grouting design where the number of expected deformation zones encountered in the tunnel is 7 or less in SD3. This is according to the number of interpreted weakness zones in this domain given the geological prognosis (Trafikverket, 2021a). Likewise, alternative A2 refers to a more conservative grouting design where the number of expected deformation zones is 12 or less in SD3.

Normally, the objective function value would be calculated as a difference between the benefit of an alternative and its corresponding construction costs and associated risk costs, but since both alternatives have the same benefits in a functioning tunnel, the benefit terms can be omitted. As such, the analysis will instead investigate which alternative has the smallest total cost C_{tot} which is the sum of the cost of construction and the cost of failure, see equation 5. The risk cost is in this context based on a probability of failure and the scale of the economic consequence of failure, each with associated distributions. Since these terms are dependent on their distributions, Monte Carlo

simulation with 10 000 iterations will be conducted in order to characterize the total cost, with the mean value of these total costs between results representing the two alternatives. The basic structure of the cost-benefit analysis is shown in Figure 23.

$$C_{tot} = C_{construction} + C_{failure} \quad (5)$$

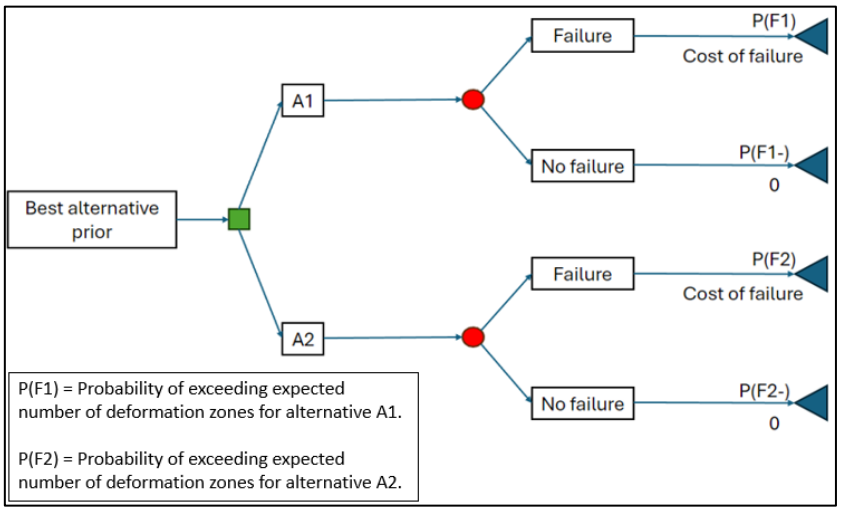

Figure 23: Structure of the cost-benefit analysis.

The construction costs have been estimated based on documentation from the Varberg tunnel project. The consequence costs have been estimated based on expert elicitation by Konstantin Spinos who has experience working in a managerial role for the "Förbifart Stockholm" project among others (Spinos, 2024). The probability of failure was estimated using geostatistical simulation. Furthermore, a virtual core drilling campaign is designed to collect further data from the model for the purpose of Bayesian updating and the value of information analysis itself.

In order to include uncertainty in the analysis and to allow for Bayesian updating, multiple of the included probabilities and values related to costs of failure have been defined as distributions rather than discrete values. Once the distributions have been established for the parameters, Monte Carlo simulation is done for purposes of analysis and comparison of the two alternatives. Before moving onto more detail in the following segments, a summary of the steps of the value of information analysis block of this project is:

1. Establish beta-distributions for the prior probability of failure based on the geostatistical model
2. Design a virtual core drilling campaign for purposes of Bayesian updating
3. Update the prior probability of failure based on the results of the virtual core drilling campaign
4. Characterize costs for the core drillings
5. Characterize costs of failure for underestimating the amount of deformation zones encountered in the construction phase
6. Run Monte Carlo analysis to characterize the prior and posterior cost of each of the two alternatives
7. Determine if the virtual data collection campaign incentivizes a change in course of action and if so, calculate the value of information based on the cost of performing the campaign in comparison to the value it provides

3.3.3. Calculation of probability of failure

Calculation of probability of failure for the two alternatives was done using the constructed geostatistical model. As mentioned in chapter 3.2.1.1, it is of interest to perform the calculation in a manner that the probability of failure is on the form of a Beta-distribution P(θ|alpha,beta), as that enables Bayesian updating to be performed simply by adding new values for alpha and beta from any further data collection in order to update the probability (Clyde et al., 2022).

After isolating the cells corresponding to the tunnel segment in SD3, this amounts to a total of 2674 cells. In order to estimate the probability of failure for alternative A1 and A2, two Beta-distributions were calculated using the cells. The first distribution describes the probability of more than 7 deformation zones being encountered in these cells, while the second distribution describes the probability of more than 12 deformation zones occurring. The method for calculation of these distributions is a for-loop run for all cells constituting the tunnel, where each cell has its given probability of giving a deformation zone. However, this method has two problems.

- The geostatistical model contains a lot of noise
- Deformation zones are continuous, and take on the appearance of large fields of increased probability in the model

Without accounting for the noise nor the continuity of deformation zones in the model, an overestimation of the number of deformation zones in the tunnel is to be expected. As such, two parameters were introduced to account for these two issues.

In order to account for the presence of noise, a threshold value was introduced where any cell with a corresponding value below the threshold value would instead be set to zero. In order to account for uncertainty in both the model and the parameter itself a uniform distribution was used to represent this threshold parameter. The minimum value of 0.10 corresponds to the mode value for all cells and is regarded as a background noise for the model, resulting from the prevalence of a large number of singular deformation zone cells disconnected from larger patterns between simulations. The maximum value of 0.5 is an arbitrary value picked to represent a clear consistency in the model to generate a deformation zone in the cell.

As for the issue of continuity in the model, a buffer was introduced where in any instance during the for-loop of the tunnel a deformation zone being encountered, the loop would skip the following cells to account for continuity and to make sure that no single deformation zone would be counted multiple times. This buffer would thereby consider the overlap of closely occurring continuous deformation zones between different simulations in SGeMS and was therefore named the SCOOB-number (Simulation Continuity Overlap Occurrence Bypass-number) for the purposes of this project. The function of the SCOOB-number is illustrated in Figure 24. A uniform distribution was adapted for this parameter as well in order to take uncertainty into account, with a value ranging between zero and two hundred cells skipped as the width of the probability fields in the model tend to take on a value in this range. This effect is best observed in Figure 35 showcasing how the cells with high probability of deformation zone appear in clusters.

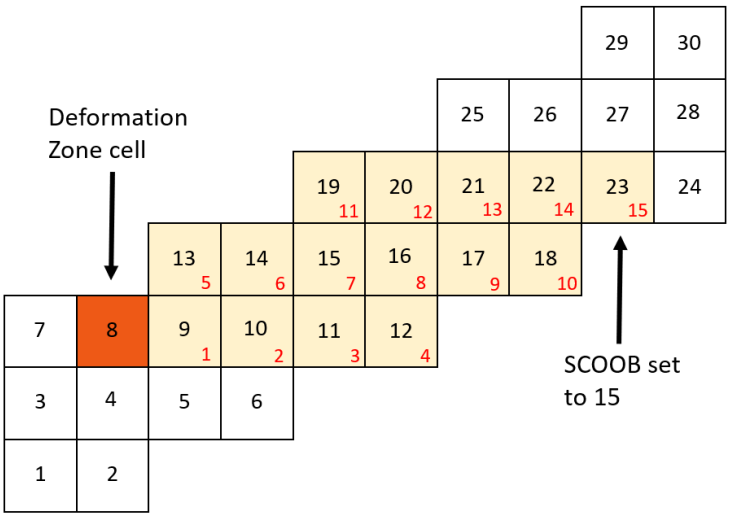

Figure 24: Illustration of how the SCOOB-number functions. All yellow cells, coming after the deformation zone cell, numbered 1 through 15 are skipped.

Given the two parameters, the general procedure for calculation of the probability of failure is:

1. Isolate the cells in the model relating to the tunnel
2. Sort the cells in order of start of tunnel to end of tunnel
3. Generate a threshold value from the distribution unif(0.1,0.5) and set all cell values below the threshold to zero
4. Walk through the N tunnel cells where every cell has their corresponding probability of adding a deformation zone to the counter. If a deformation zone is encountered a number of the following cells to be skipped is generated by unif(0,200) (according to the SCOOB-number)
5. The counter for number of deformation zones is saved before being reset
6. Monte Carlo simulation is done by repeating steps **3** through **5** 10 000 times
7. A beta distribution is constructed by setting alpha to the number of times 7 deformation zones was exceeded for A1 and to the number of times 12 was exceeded for A2, with beta being the number of times the values were not exceeded. These beta distributions describe the probability of respective number of deformation zones being exceeded in the tunnel and as such the probability of failure for each alternative.

3.3.4. Bayesian updating

In value of information analysis, the next step behind establishing the basic structure of the cost benefit analysis and the prior probability is to perform Bayesian updating. Through Bayesian updating, the impact of a data collection campaign can be estimated by performing a virtual data collection campaign and updating the prior probability into a pre-posterior probability and investigating the difference in costs (Freeze et al., 1992).

In the context of this project, this virtual data collection campaign is conducted by performing further virtual core drillings and calculating the expected number of deformation zones that would be encountered in the tunnel based on the findings in these. The idea behind this methodology is based on the assumptions that the quality of the model is better closer to the surface (this assumption is further motivated through findings presented in section 4.1 - “Results from the geostatistical simulation”), and that the general occurrence or concentration of deformation zones-

the number of deformation zones per unit volume that is- does not vary much with depth in crystalline rock (Seeburger & Zoback, 1982). Following this reasoning, a virtual data collection campaign of core drilling investigations following the tunnel on the surface of the model ought to be a way of collecting additional data that can be used for Bayesian updating of the probability of failure. For sake of simplicity, these virtual core drillings are done vertically and in order to remain consistent with the methodology behind the calculation of the prior probability of failure, the threshold distribution and SCOOB-number distribution are also applied in this case.

The general procedure for conducting the virtual core drillings and the Bayesian updating of the prior probability is:

1. Extract the cells corresponding to the surface of the tunnel down to the warranted depth of the virtual core drillings
2. Define the amount of virtual core drillings that are to be done
3. The set amount of virtual core drillings are done in random locations in the defined area above the tunnel
4. A mean value is calculated using the values from cells encountered in the virtual core drillings
5. A virtual tunnel is defined as N number of cells, all with the value of the mean from the core drillings
6. These tunnel cells are checked one by one, being set to 0 if exceeded by a random number from the distribution unif(0.10,0.5) (threshold value) and skipping a number of cells equal to a random number unif(0,200) (SCOOB-number) if a deformation zone is encountered after adding it to the counter
7. The counter for number of deformation zones is saved before being reset
8. Monte Carlo simulation is done by repeating steps **3** through **6** 10 000 times
9. A beta distribution is constructed by setting alpha to the number of times 7 deformation zones was not exceeded for A1 and to the number of times 12 was not exceeded for A2, with beta being the number of times the values were exceeded.
10. The Bayesian updating is done by yet another Monte Carlo simulation. A pre-posterior probability distribution is constructed by pulling values from the beta distribution describing prior probability of failure and the new beta distribution from the virtual core drilling campaign. The values are then inserted into equation 6, which is derived from applying equation 4 to the context of the project.

$$P(F|D^-) = \frac{P(F)P(D^-|F)}{P(F)P(D^-|F) + P(F^-)P(D^-|F^-)} \quad (6)$$

Where:

$P(F|D^-)$ is the updated probability of failure given that the number of detected deformation zones is lower than 7 or 12 in the virtual sampling campaign, for alternatives A1 and A2 respectively.

$P(F)$ is the prior probability of failure.

$P(D^-|F)$ is the probability of detecting less than 7 or 12 deformation zones in the virtual campaign given that at least 7 or 12 deformation zones exist in the tunnel geometry, for alternatives A1 and A2 respectively.

$P(F^-)$ is the probability of no failure

$P(D^-|F^-)$ is the probability of detecting less than 7 or 12 deformation zones in the virtual campaign given that the number of deformation zones in the tunnel geometry is less than 7 or 12, for alternatives A1 and A2 respectively.

3.3.5. Estimation of costs

In the context of this project, the construction cost refers to the base, establishing cost of each of the two grouting alternatives without any added risk. This cost has been exemplified based on costs for different grouting methods from a cost analysis of the Varberg tunnel project (received as an excel-document from the project manager). Two grouting methods have been considered while estimating the construction cost- one expensive alternative adapted for transmissive rock (referred to as injection class 3a) and one cheaper alternative for general usage (referred to as injection class 1). The difference between the two alternatives used for analysis relates to the extent of which the more expensive grouting method has been applied throughout the tunnel. For A1, 7 screens worth of the expensive grouting method has been taken into account, whereas for A2, 12 screens worth have been taken into account. In order to calculate the costs themselves, the length of these higher quality screens have been subtracted from the total length of the tunnel whereafter the rest of the tunnel can be assumed to be using the cheaper grouting method, and the cost can be calculated given a cost of respective grouting method in SEK per meter. The costs per meter for the two injection classes considered are presented in Table 3. All constituting parts as well as the costs for alternatives A1 and A2 are presented in Table 4.

Table 3: Costs for the different injection classes considered.

Injection class	Cost [SEK/m]
1	32 302
3a	60 155

Table 4: All constituting parts making up the total construction costs for alternatives A1 and A2. As mentioned in section 3.2.4, only SD3 have been fully modelled and considered in the final analyses.

Parameter	Value
Length of tunnel stretch SD3	2683 [m]
Cost injection class 1	32 302 [SEK/m]
Cost injection class 3a	60 155 [SEK/m]
Length of screen injection class 3a	24 [m]
Meters of injection class 3a for A1	168 [m]
Meters of injection class 1 for A1	2515 [m]
Total construction cost A1	**90 674 065 [SEK]**
Meters of injection class 3a for A2	288
Meters of injection class 1 for A2	2395
Total construction cost A2	**94 048 465 [SEK]**

In order to gain input for the consequence cost of encountering more deformation zones than expected in the construction phase an interview was conducted. The interviewee Konstantin Spinos is an experienced project manager and has worked on the similar tunnelling project “Förbifart Stockholm” among others. In accordance with guideline material for conducting interviews with experts, focus was put on establishing an upper bound, lower bound and expected value for the different parameters discussed (O’Hagan, 2019). This was done to properly account for uncertainty

in the values estimated. These estimated bounds and modes were thereafter used to establish distributions for each of the different parameters. The parameters, their associated distributions and their associated values are shown in Table 5. The interview of Konstantin Spinos was done in a way to first establish the consequences of encountering more deformation zones than expected, and thereafter quantify these consequences using bounds and an expected value as earlier discussed.

Table 5: Parameters associated with consequence costs and their respective distributions.

Parameter	Associated distribution	Associated value
Cost in SEK per day of construction stop	Triangular	Min: 300 000, mid: 550 000, max: 700 000
Number of days of stopped construction due to unexpected deformation zone	Triangular	Min: 1, mid: 2, max: 4
Probability of 3 days construction stop for rock reinforcement measures due to bad quality of rock	Uniform	Min: 5%, Max: 30%

According to Spinos (2024), the main possible consequences of encountering additional deformation zones as framed in the context of our project would be twofold; the time delay caused by needing more intensive grouting measures and the potential time delay if the rock quality is low enough as to require additional reinforcement measures (Spinos, 2024). The former consequence of needing additional grouting measures can be assumed to always result in a delay as a deformation zone will mostly always require at least some amount of extra grouting to keep in line with hydraulic requirements for the tunnel. This additional grouting would take at least one day since a single screen requires at least that amount of time to harden, whereas in the worst case, multiple injections might be required over time leading to up to four days of delay. The other consequence related to bad quality rock would be the possible need for reinforcement. In case of a large deformation zone with low quality rock, additional reinforcement might be needed using rock bolting, where steel rods are inserted into the fractured rock mass to improve stability (Spinos, 2024). Having to resort to reinforcing of the rock is in the context of this project always considered to cause a three-day delay, and the probability of any given deformation zone necessitating further reinforcement is set to a uniform probability distribution between 5-30%. Both consequences result in delays which implies that the entirety of the construction project must come to a halt while the issues are being addressed (Spinos, 2024). Having all equipment and personnel on standby results in an estimated cost of around 550 000 SEK per day for a project of this size, with a lower and upper bound of 300 000 and 700 000 respectively (Spinos, 2024). In the context of this project, the costs associated with these consequences have been assumed to relate to this cost of having to halt the project only. Any additional costs associated with the handling of the consequences such as the rock bolting or additional injection measures have not been considered.

It is important to note that this number of extra days required is based on the number of deformation zones encountered above the predicted amount. As such, another input parameter aside from the cost per day and amount of days per deformation zone is the number of additional deformation zones encountered when failure occurs. To evaluate this parameter, additional distributions were built using the results from the evaluation of probability of failure. This was done by constructing Pearson-distributions using the results from the Monte Carlo simulations and the pearspdf function, with number of deformation zone cells surpassing 7 and 12 respectively for the

alternatives A1 and A2. A lesser problem is that these distributions can assume values below zero, but this was fixed by means of a conditioning statement that skipped negative values.

3.3.6. Calculating value of information

Once all distributions related to costs of failure and probability of failure have been calculated, Monte Carlo simulation was performed to compare the two alternatives and their expected costs. As earlier established, an additional data-collecting campaign is only worth performing if it provides incentive to make a different decision than what would be done without it, and if the costs of performing the campaign are less than the value of the information that it provides. In the context of this project, this means that the investigation is worth performing if the Bayesian updating shows a different alternative as having the lower expected cost than what could be expected looking at the prior alternatives, and that the difference in expected cost between the better alternative during prior analysis and posterior analysis is higher than the cost of performing the campaign.

The cost of performing additional core drillings is within this project based on estimates from email contact with experts. Table 6 showcases the different constituents making up the total cost of performing additional core drilling investigations.

Table 6: Constituents making up the total cost of the additional core drilling investigations.

Core drilling actions	**Costs**
Establishing [SEK]	25000
Pre-drilling + piping [SEK/m]	3000
Setting-time concrete [SEK/core drilling]	20000
Core drilling [SEK/m]	1500
Measurement of deviation [SEK/core drilling]	7000
Waypoint markings [SEK]	18000
De-establishing [SEK]	10000
Treatment of drill cuttings [SEK/core drilling]	35000
Storage boxes [SEK/m]	50
Moving between positions [SEK/core drilling]	2500
Totals	
Base cost [SEK]	53000
cost per meter of drilling [SEK/m]	4550
cost per core drilling [SEK/core drilling]	64500

As such, the total cost of performing a campaign involving **A** number of core drilling tests to a depth of **B** meters is as equation 7:

$$Total\ cost\ of\ campaign\ in\ SEK = 53\,000 + A * B * 4550 + A * 64500 \quad (7)$$

And the value of information can be calculated and deemed useful if the better alternative changes between the prior and posterior analysis and:

$$Cost_{preposterior} - Cost_{prior} > Total\ cost\ of\ campaign\ in\ SEK$$

3.4. Sensitivity analysis

Given that the methodology introduces two different entirely new parameters related to the characterization of the number of expected deformation zones, it is of high importance to determine their respective resulting impact in that regard. Also, since generating a large number of model realizations can be highly time consuming, it is of interest to evaluate just how many realizations should be generated before reaching a steady state in terms of the probability-based model. Finally, yet another topic of interest is to analyse the impact that the number of separate core drillings will have on the pre-posterior analysis. Only one version of a core drilling campaign was used to generate the results whereafter different numbers were tested to determine the overall impact. Since changes to all of these different parameter and choices of values could have a large impact on the results, conducting sensitivity analysis to check to which extent the choices made impact the results becomes of high interest. The most basic method of performing this kind of sensitivity analysis is the direct method, where prior assumed values are substituted with new values to see the impact on the results (Vipond, 2024).

To perform sensitivity analysis on the number of model realizations, probability-based models of different numbers of realizations were checked in regard to the impact on the distribution of probability of deformation zone for cells in the tunnel. While the default number of realizations used in analysis was 200, the sensitivity analysis also checks combinations of 10, 40, 100 and 300 realizations.

As for the number of core-drillings, it was of interest to evaluate the impact of number of core drillings on the pre-posterior probability of failure. While the default number used for analysis was 10 core drillings, values of 3, 5, 20 and finally the extreme case of 100 were checked to investigate the behaviour of the probability of failure in regard to changes in the number of core drillings.

For the SCOOB-number and the threshold value, distributions were defined to take uncertainty into account. In order to preserve the manner of which uncertainty is represented in these parameters, sensitivity analysis was done by multiplying their corresponding distributions with different scaling-factors. The scaling-factors used for this purpose was 0.5, 1.5 and 2. Setting each parameter to zero was also done to investigate the total effect of introducing these parameters have on the resulting number of deformation zone cells.

4. Results

All results regarding the geostatistical simulation modelling, and the performed VOIA is presented in the following subsections. Regarding the geostatistical simulation, topics such as the quality of the model in different aspects are presented and described, and further discussed in the discussion section. Aspects of the final geostatistical model that are problematic, such as the high level of noise and the continuity of deformation zones within the cells associated with the tunnel, have been noted and considered in the analyses. The results regarding the prior and pre-posterior analyses are complemented with a brief sensitivity analysis. In the sensitivity analysis, the variability and influence of uncertain parameters associated with the VOIA is examined.

4.1. Results from the geostatistical simulation

An overview of the finalized probability-based geostatistical model at structure geological domain 3 is presented in Figure 25. As seen in the left-side part of the figure, parts of the finalized model do not include any distinct deformation zone information. The part of the model clearly influenced by conditioning data has been highlighted and presented more closely together with a representation of the planned tunnel geometry. The left and middle pictures in Figure 25 are representing the top of the simulation grid (top of the bedrock), and the right-side picture is representing a cross section of the model at a depth of 30 meters - showcasing the tunnel. Note that this is not the planned depth of the tunnel. The tunnel geometry shown is only constructed for visualisation purposes.

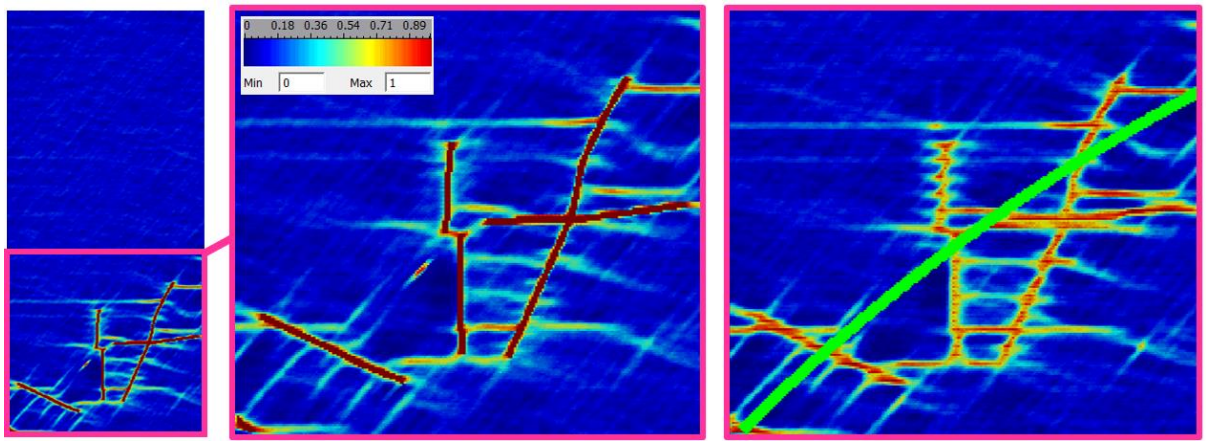

Figure 25: Overview of the finalized probability-based geostatistical model, constructed using the SGeMS software. The green line in the illustration to the right represents the tunnel.

A main objective regarding the multiple point statistics method was to create a geostatistical model that reconstructs patterns included in the selected training image. A first evaluation of the applicability of the method used (including selection of input parameter values etc.) is to compare the outcome of the simulations with the training image used. In general, the extent to which the simulation algorithm reconstructs patterns seen in the training image indicates the quality of the simulation performed. Since this analysis is made on a three-dimensional grid, the quality of the simulation outcome can be analysed in both the horizontal and the vertical directions. Investigating the influence of different input parameters in the SGeMS software through trial simulations implied that an increased simulation quality in one direction would lead to a decrease in quality of the other. Because of this, a prioritization between the two directions had to be made. The final selection of input parameter values resulted in simulations performing better in the horizontal direction than in the vertical. The choice to prioritize the horizontal quality was made for the purpose of easier

visualisation and visual monitoring of the repetitional tendencies among the many simulation iterations performed. The reconstruction of patterns included in the training image, in the horizontal and vertical directions for the input parameter values used, is exemplified in Figure 26 and Figure 27 respectively.

As seen in Figure 26, several continuous lines with strike around 230° is including deformation zones in approximately 40% of the realizations. This is a distinct reconstruction of a pattern seen in the excerpt of the training image presented in Figure 26, that also has several continuous deformation zones in the same strike. The distances between the proposed deformation zones seem to follow some tendency, since they all are in the same magnitude. However, the distances between them are not really a reconstruction of the ones defined in the training image. Since the excerpt of the training image, and the simulation result in Figure 26 are in the same scale, comparing the two suggests that the distance between deformation zones is around 1/3 in the simulations compared to the training image. Apart from these 230° deformation zones, also the 90° strike deformation zones reappear in the simulations with a distinct tendency in this example. In general, the reconstruction of patterns in the horizontal direction is good, with simulations resulting in long and continuous (often several hundred meters long) deformation zones.

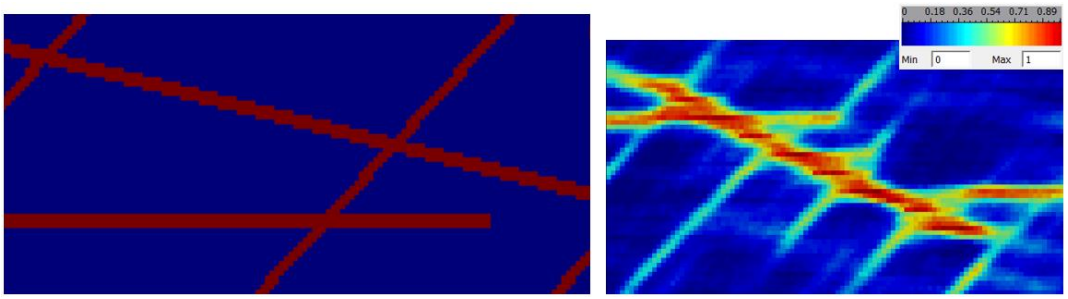

Figure 26: Example of pattern reconstruction in the horizontal direction. An excerpt of the training image is presented on the left side, and an example of the simulation result at 30 meters depth is presented on the right side.

The reconstruction of patterns in the vertical direction is not as distinct as in the horizontal direction. It is possible to notice a slight tendency regarding the dips of deformation zones following the ones defined in the training image. Here, what is notable is rather the overall tendency of proposed deformation zones having a dip towards east/west and north/south than reconstruction of defined dips in terms of degrees. One thing that is concerning is that the influence of hard data, e.g. pre-defined deformation zones at the surface, is not reaching lower than around 9 cells/90 meters. Since the distance between the ground level and the tunnel level is varying from approximately 10 to 120 meters within the analysed region, the conditioning data at the surface do not have any influence on parts of the tunnel located at large depths.

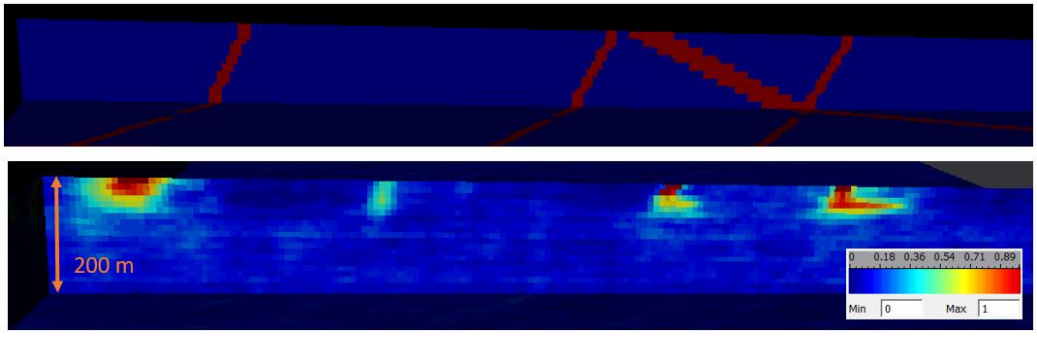

Figure 27: Example of pattern reconstruction in the vertical direction. The training image is presented at the top, and an example of the simulation result is presented at the below.

In addition to the hard data at the surface, there are cells at depths that are defined as deformation zones, according to the core drilling investigations performed. Examples of simulation results around cells defined as deformation zones according to performed core drilling investigations are presented in Figure 28 a-d. As seen in Figure 28 a-c, the 230° strike which is included in the training image is reconstructed with differing intensity as an extrapolation of the core drilling data. In Figure 28 c, the simulations tend to also create a continuous deformation zone at a strike of 280°. This strike is also present in the training image but to a smaller extent, which may be an explanation to it not appearing as often in the simulation results. Furthermore, Figure 28 c exemplifies a crossing of the two strikes, which is occurring in several parts of the training image. Figure 28 d on the other hand exemplifies a pre-defined deformation zone that is not influencing the surrounding cells in the simulations.

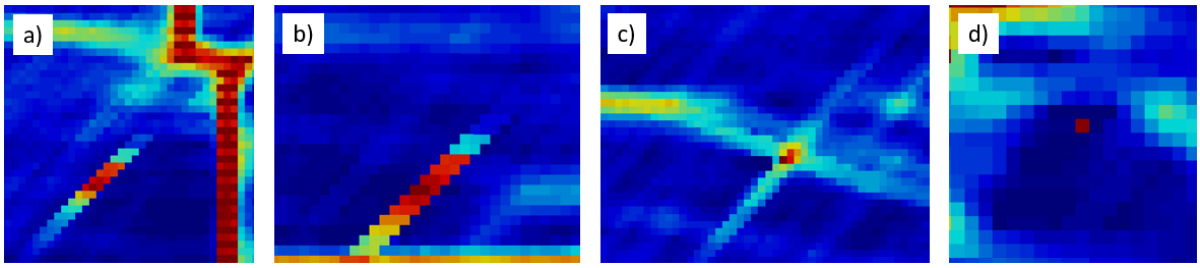

Figure 28: : Examples of simulation results around cells defined as deformation zones according to performed core drilling investigations. Pre-defined deformation zone cells are appearing as red, and their influence on surrounding areas differ.

The area surrounding the pre-defined deformation zone cell show in Figure 28 c is illustrated in a wider perspective in Figure 29. This illustration showcases an example where a crack simulated due to a pre-defined deformation cell merges with another simulated crack. Unlike what is seen in Figure 28 b, where a hard data induced crack merges with another crack with a sharp angle, the one seen in Figure 29 appears to bend towards another crack before merging. This suggests that the SNESIM algorithm used for the simulations can connect hard data points even at large distances.

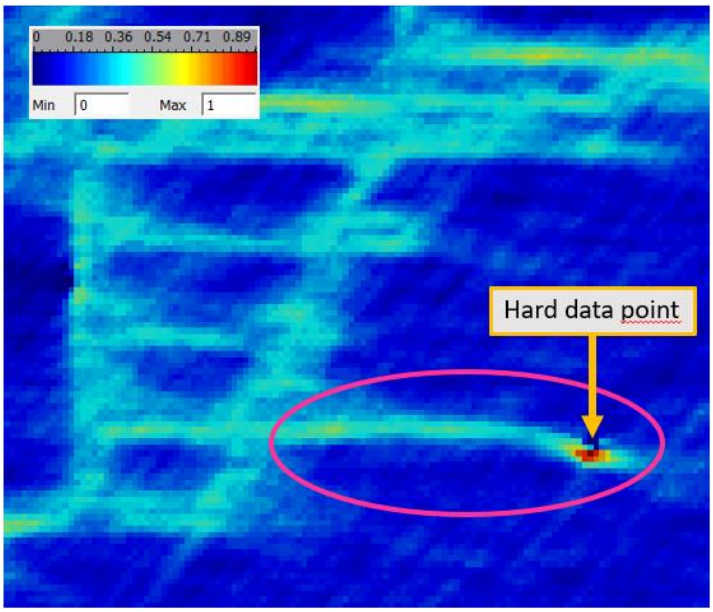

Figure 29: Example of a crack simulated due to a pre-defined deformation cell merging with another simulated crack. The figure illustrates a depth of 60 meters.

The reconstruction of the training image can be interpreted in other aspects than patterns. One of them being the concentration of deformation/non-deformation zone cells. Comparing proportions of deformation/non-deformation zone cells in the training image and simulations gives an indication on the simulation quality. If the simulation is of good quality, the distribution of deformation/non-deformation zone cells would be similar for the training image and the simulation result. Histograms on the concentration of deformation/non-deformation zone cells have been constructed for the training image used, and a simulation realization example for illustration (Figure 30). The histograms show that approximately 8% of the cells in the training image are defined as deformation zone cells, whereas this number is approximately 11% for the simulation realization example.

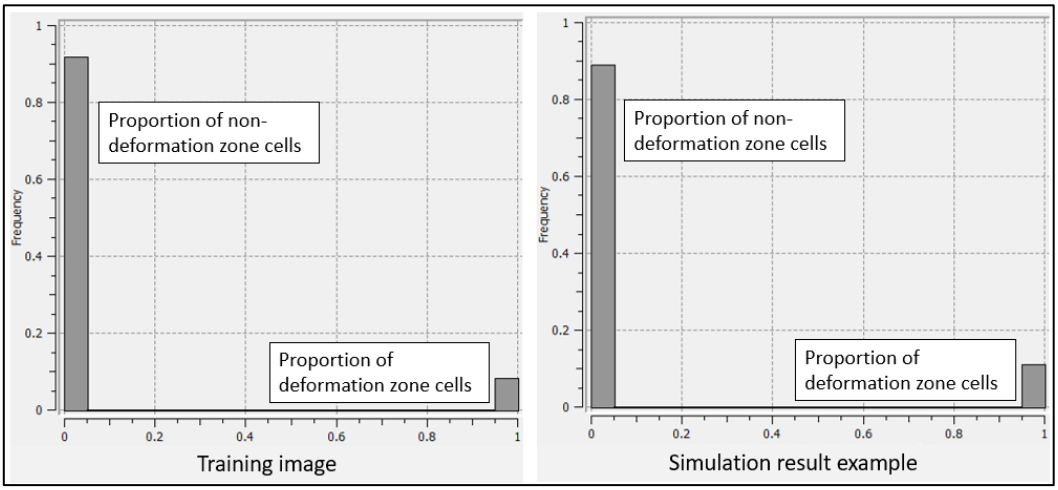

Figure 30: Histograms showing the proportion of deformation/non-deformation zone cells included in the used training image and a simulation result example.

Additionally, Figure 31 shows a histogram that presents the variation in deformation/non-deformation zone cell proportions among all 200 simulation realizations. The histogram shows a skewed distribution with mode around 0.112, upper limit around 0.123 and a lower limit around 0.102.

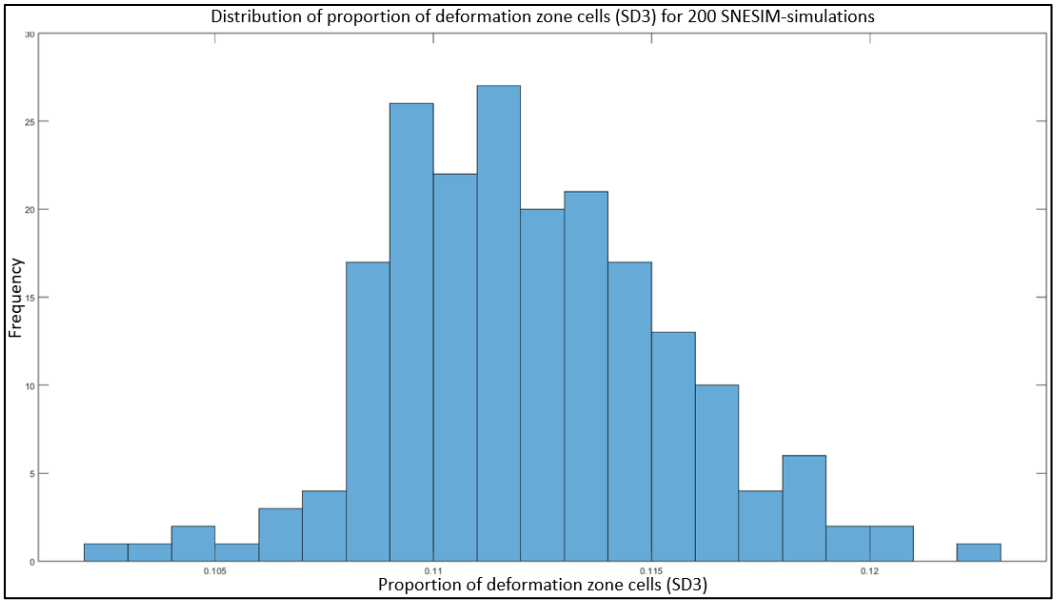

Figure 31: Distribution of proportion of deformation zone cells (SD3) for 200 SNESIM-simulation realizations.

As seen in all figures showcasing the model, there is a distinct level of noise. This is especially visible in the parts far from the conditioning data, i.e. in the northern part of SD3 (the upper part of the left side image in Figure 25). To visually examine both the level of noise in the model, and the certainty of simulated deformation zones, the minimum and maximum values for visualisation can be adjusted. In Figure 32, three different minimum values are illustrated, i.e. 0.1, 0.2 and 0.5. Showcasing these different minimum values gives indications regarding e.g. relevant threshold values for further analyses, and the overall quality of the model. With the minimum value set to 0.1, there is still a large amount of noise over the whole model. At 0.2, most of the obvious noise is removed. Deformation zones simulated in at least 50% of all 200 realizations are shown in the image illustrating a minimum value of 0.5, indicating that there would likely be deformation zones at the visible locations according to the model.

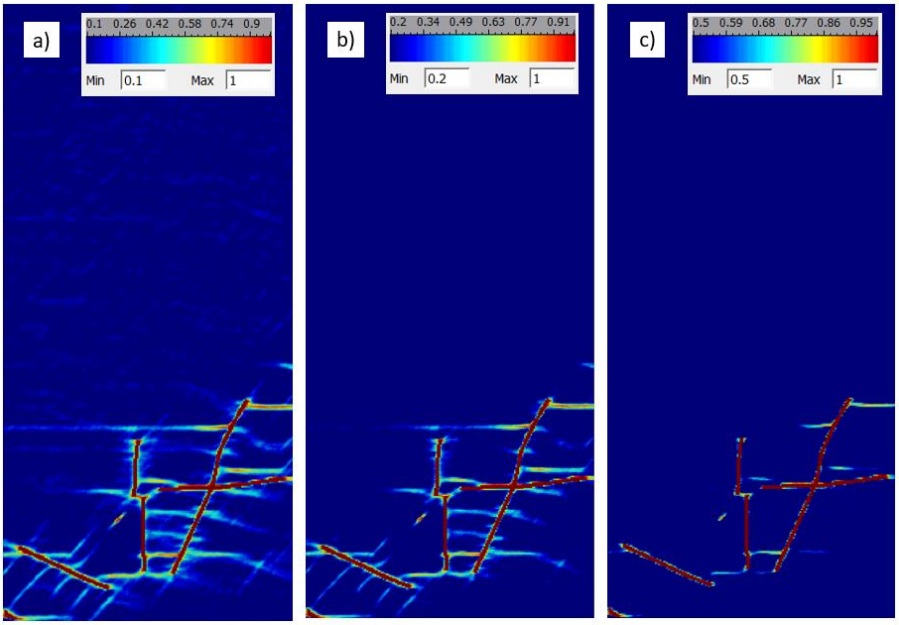

Figure 32: Different minimum values selected for visualisation in SGeMS. All three illustrations represent the top layer of the model. Minimum values selected: a)=0.1, b)=0.2, c= 0.5.

Ultimately, the constructed model is used as analysis material regarding probability of deformation zones and associated implications at the tunnel. In the context of this project, the simulated probabilities for the specific simulation grid cells intersecting with the tunnel are used in the CBA and VOIA. Figure 33 shows an example of what is to be analysed in further work in the CBA and VOIA, namely the probability of deformation zones appearing in simulation grid cells intersecting with the tunnel.

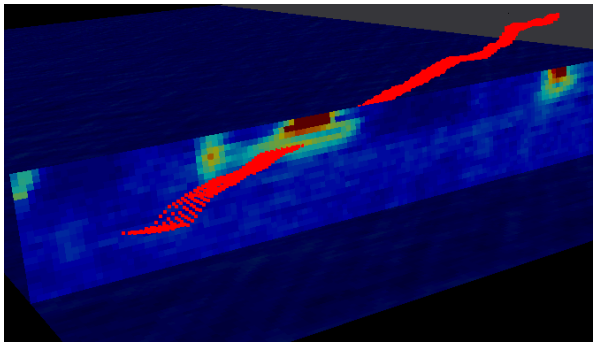

Figure 33: Example of the tunnel intersecting with simulation grid cells with probable deformation zone.

4.2. Results from VOIA

The results from the value of information analysis are presented in the following subsections. Firstly, the results of the prior analysis and the associated probability distributions are presented. The results of the Bayesian updating, and the recalibrated probability distributions are presented in the pre-posterior analysis section.

4.2.1. Prior analysis

Results related to the prior analysis includes the extraction of tunnel intersecting cells belonging to SD3 for analysis, the calculation of beta-distributions for the two alternatives and the cost-benefit analysis using the prior probability of failure.

In Figure 34 , the distribution of probability of deformation zone in the 2674 cells after compiling the 200 SNESIM-simulations is shown. Only a small fraction of the cells has a probability of deformation zone above 40%. The mode probability value is 10% while the mean probability value is 14%.

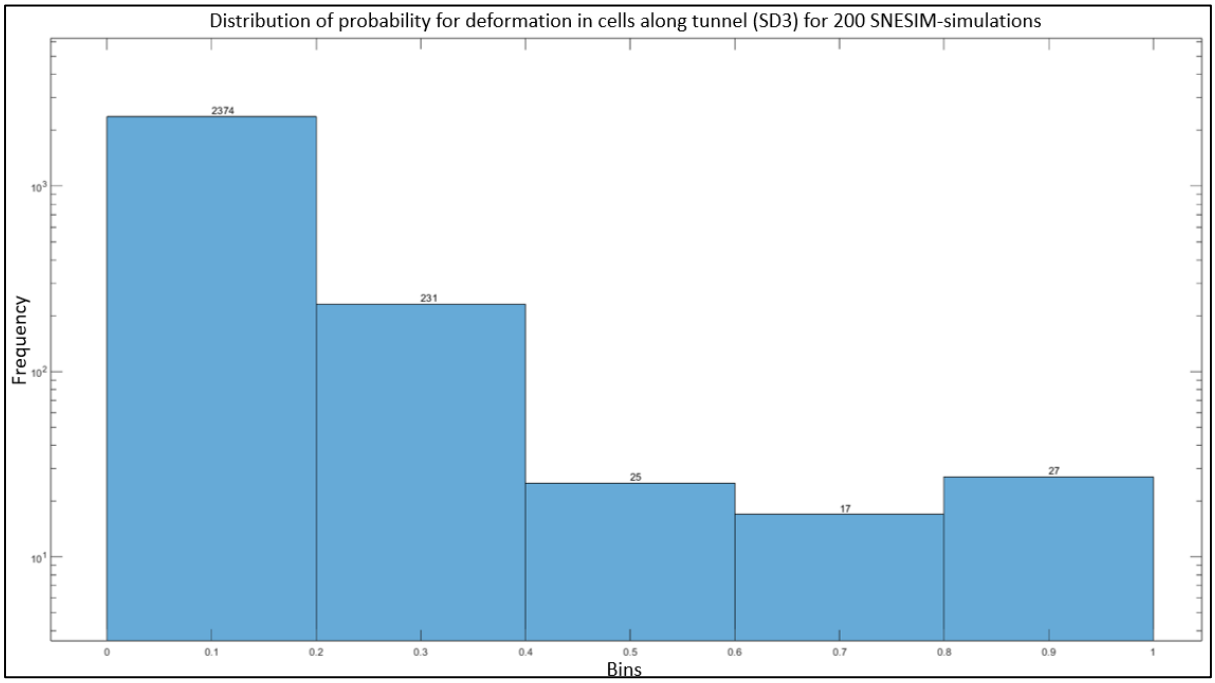

Figure 34: Distribution of probability for deformation in cells along tunnel (SD3) for 200 SNESIM-simulations.

Another aspect of interest to the analysis is the spatial distribution of these cells. After sorting the cells in order of start of the tunnel to end of the tunnel in SD3 the spatial distribution is in accordance with Figure 35. Due to the structure of the geostatistical model, there is a clear clustering effect with continuous stretches of cells with higher probability of deformation zones. The size of these clusters is the basis for the SCOOB-number used to account for the continuity of these probability fields in the model.

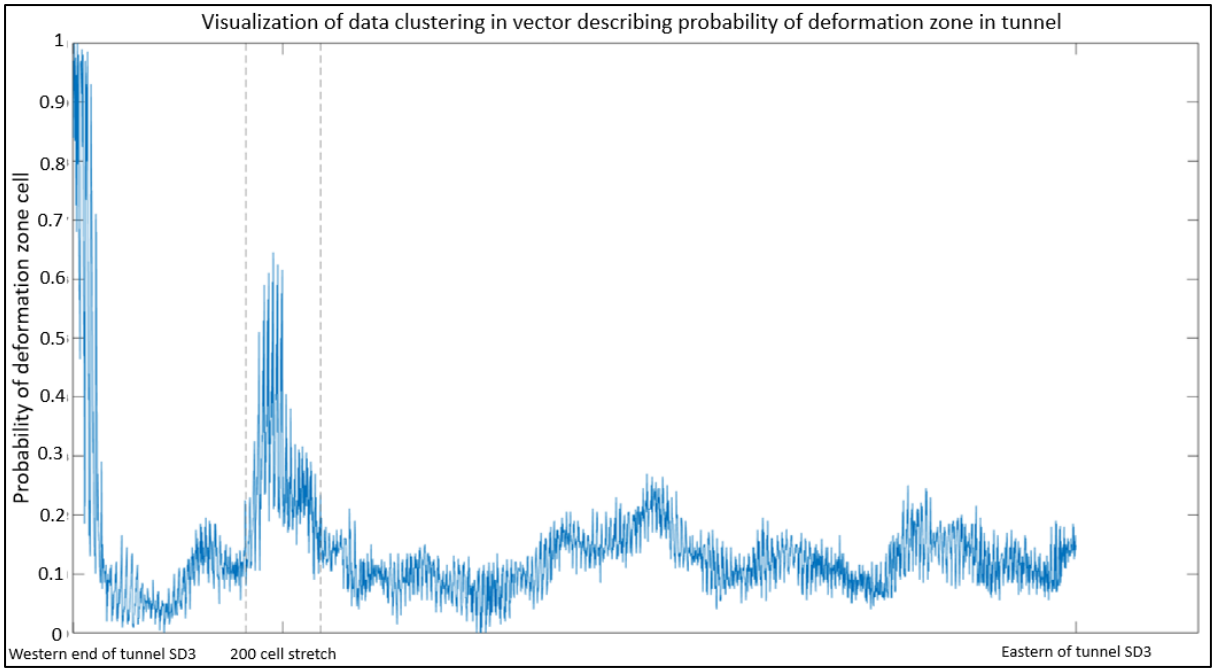

Figure 35: Visualization of data clustering in vector describing probability of deformation zone in tunnel.

One of the main results used for further analysis in the prior analysis are the beta-distributions describing the probability of failure for A1 and A2 respectively, these are showcased in Figure 36. Based on the distributions, the probability of failure ranges between around 24-27% for A1 and 17-19% for A2. The corresponding alpha and beta values were 2572 and 7428 for A1 and 1791 and 8209 for A2.

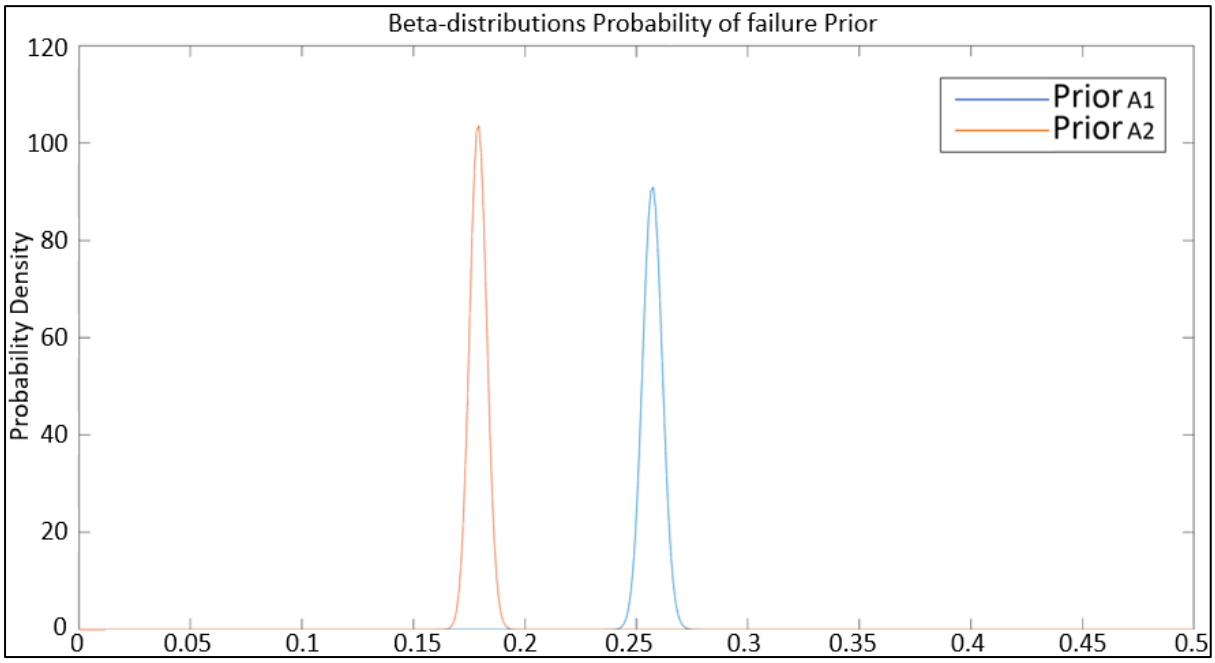

Figure 36: Beta-distributions Probability of failure Prior, for A1 and A2.

The beta-distributions shown in Figure 36 are based on Monte Carlo simulation of the number of deformation zones encountered in the extracted tunnel cells. The distribution of the number of deformation zones encountered in this Monte Carlo simulation is shown in Figure 37.

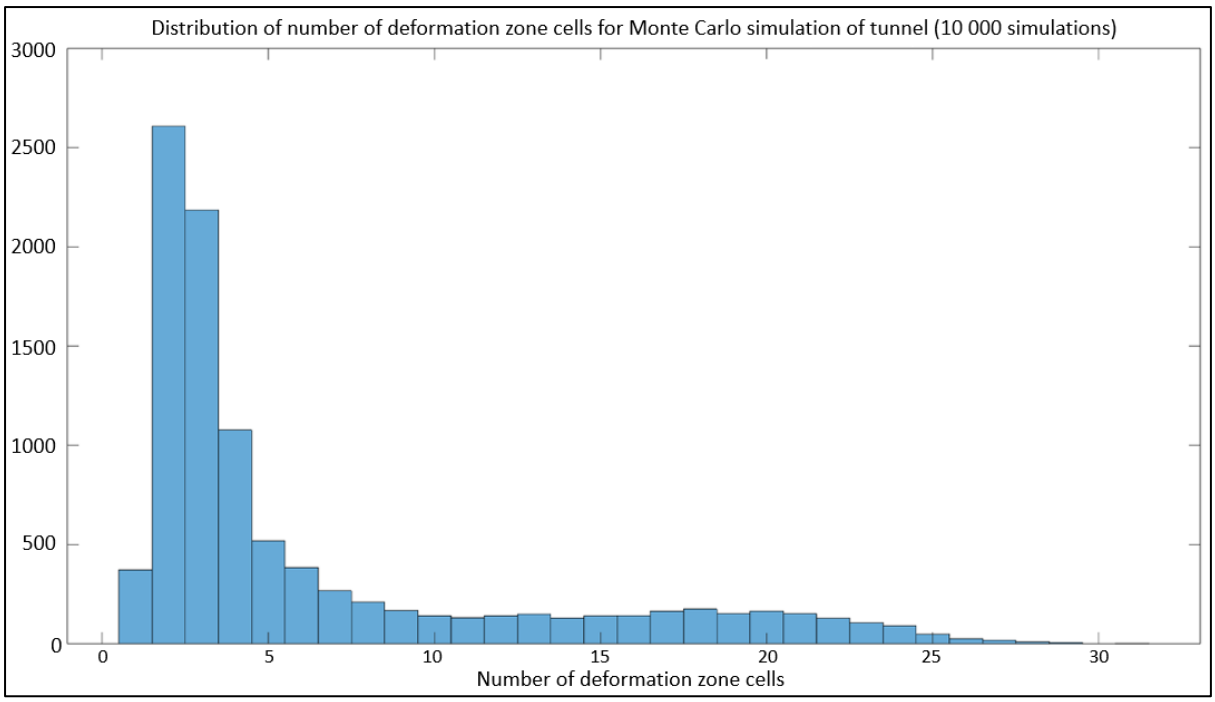

Figure 37: Distribution of number of deformation zone cells for Monte Carlo simulation of tunnel (10 000 simulations).

As can be seen in the distribution, the results of the Monte Carlo analysis are left skewed and with a high variance. The mode number of deformation zones encountered is 2 while the mean is 6.5.

Another set of distributions important for analysis are shown in Figure 38 and Figure 39. These Pearson distributions are used to generate the number of additional deformation zones encountered in the tunnel segment in SD3 when failure occurs in the CBA. The expected value for these distributions is seven for the distribution corresponding to A1 and five for the distribution corresponding to A2.

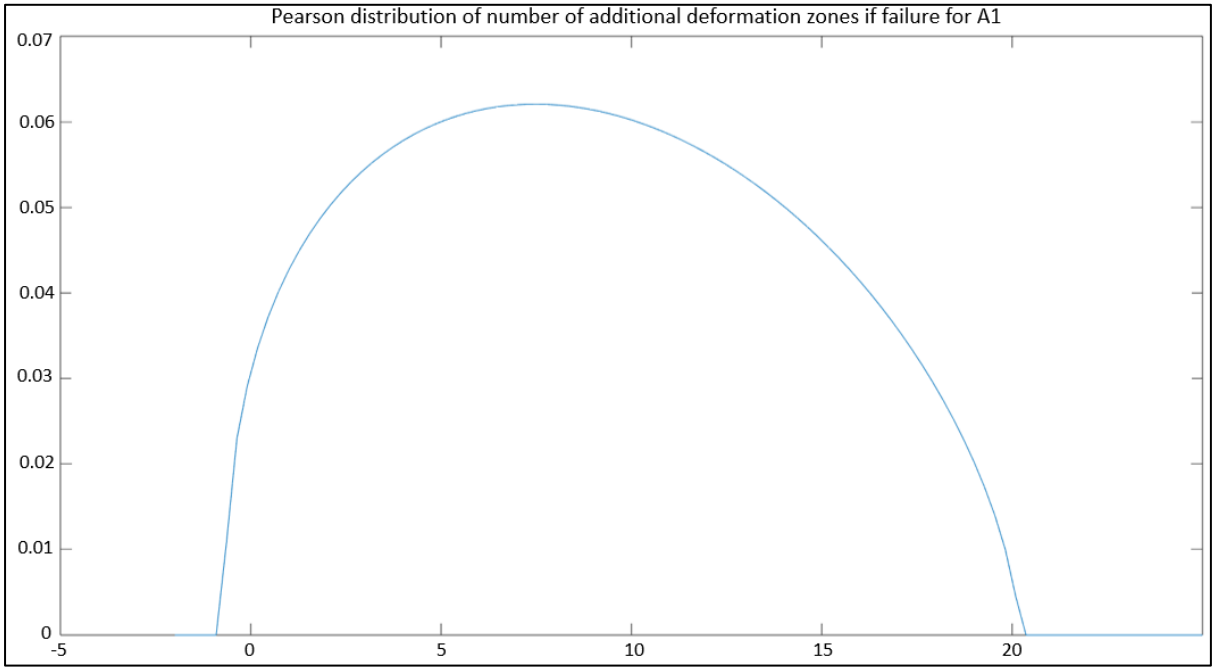

Figure 38: Pearson distribution of number of additional deformation zones if failure for A1.

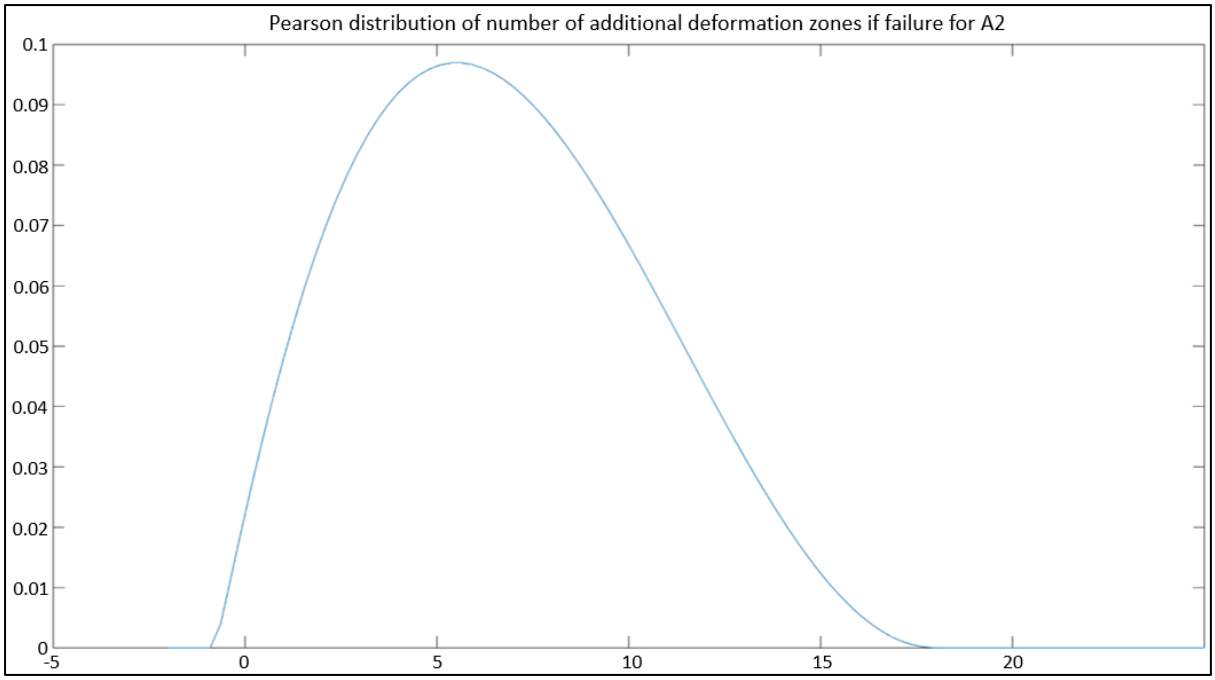

Figure 39: Pearson distribution of number of additional deformation zones if failure for A2.

To calculate the CBA results for the prior analysis using the established distributions for probability of failure and costs, Monte Carlo simulation was done with 10 000 iterations. The cost results are shown in Figure 40 and Figure 41. The mean cost of A1 is 93.48 millions of SEK and the mean cost of A2 is 95.64 millions of SEK. Showing alternative A1 to be the more economically beneficial option without additional investigations.

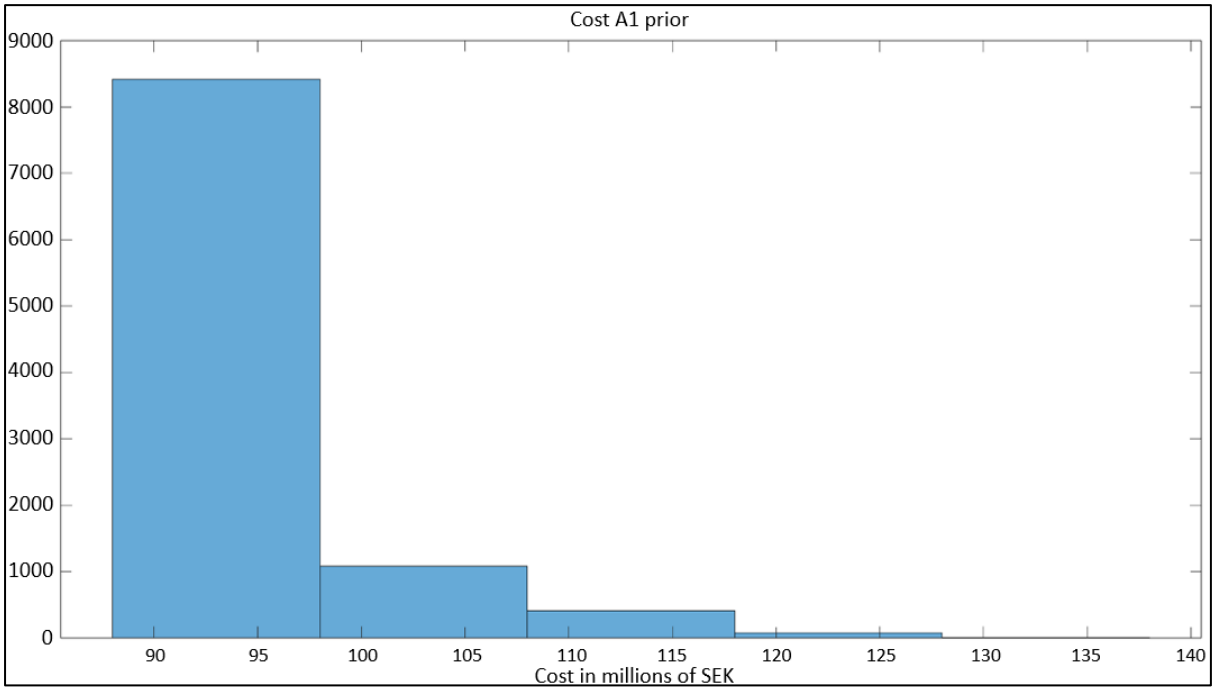

Figure 40: Cost for A1 in terms of millions of SEK in the prior analysis.

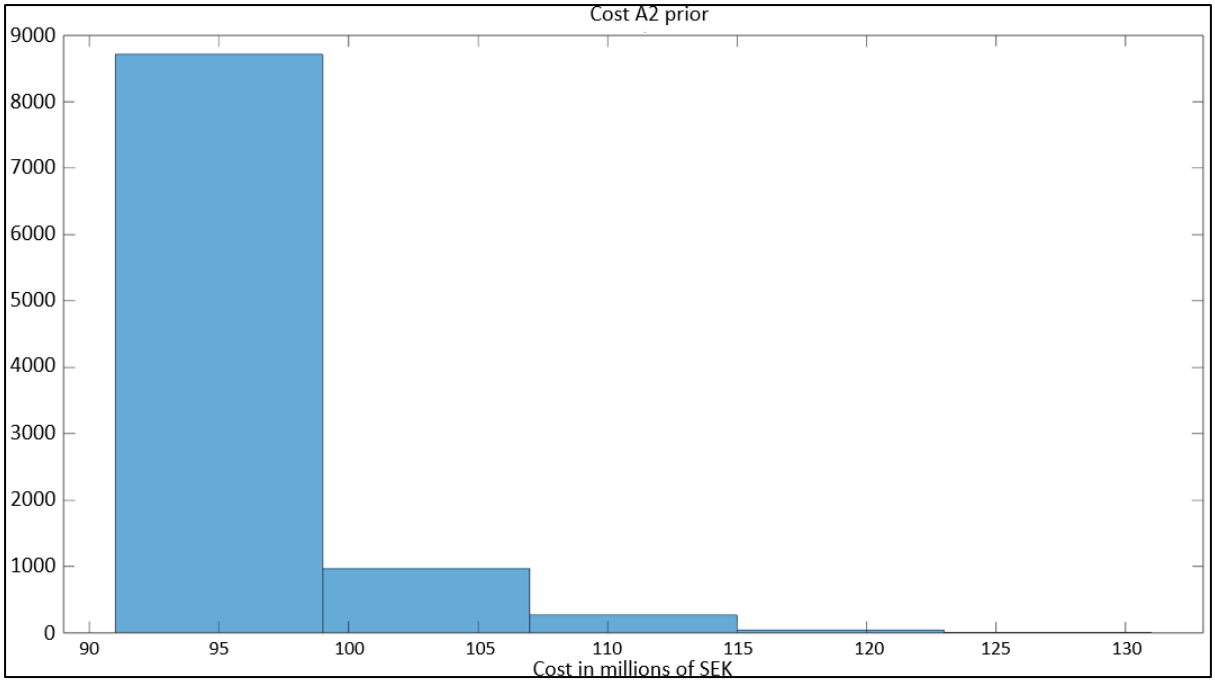

Figure 41: Cost for A2 in terms of millions of SEK in the prior analysis.

4.2.2. Pre-posterior analysis

Following the methodology in segment 3.2.3. another Monte Carlo simulation with 10 000 iterations was done where for each one a virtual tunnel was constructed and simulated. For these virtual tunnels, the probability of deformation zone was based on a virtual core drilling campaign with 10 core drilling investigations each for 5 cells in depth. Realistically a larger depth should be used for the investigations as 5 cells only corresponds to 50 meters, but a lower number was opted for since the quality of the model deteriorates with depth. The resulting alpha and beta values were 451 and 9549 for A1 and 791 and 9209 for A2. Bayesian updating of the probability of failure was done by utilizing equation 6, resulting in the distributions showcased in Figure 42. Furthermore, the distributions shown in Figure 38 and Figure 39 describing the number of additional deformation zones above the limit of failure for A1 and A2 were updated including values above the limits from the pre-posterior analysis.

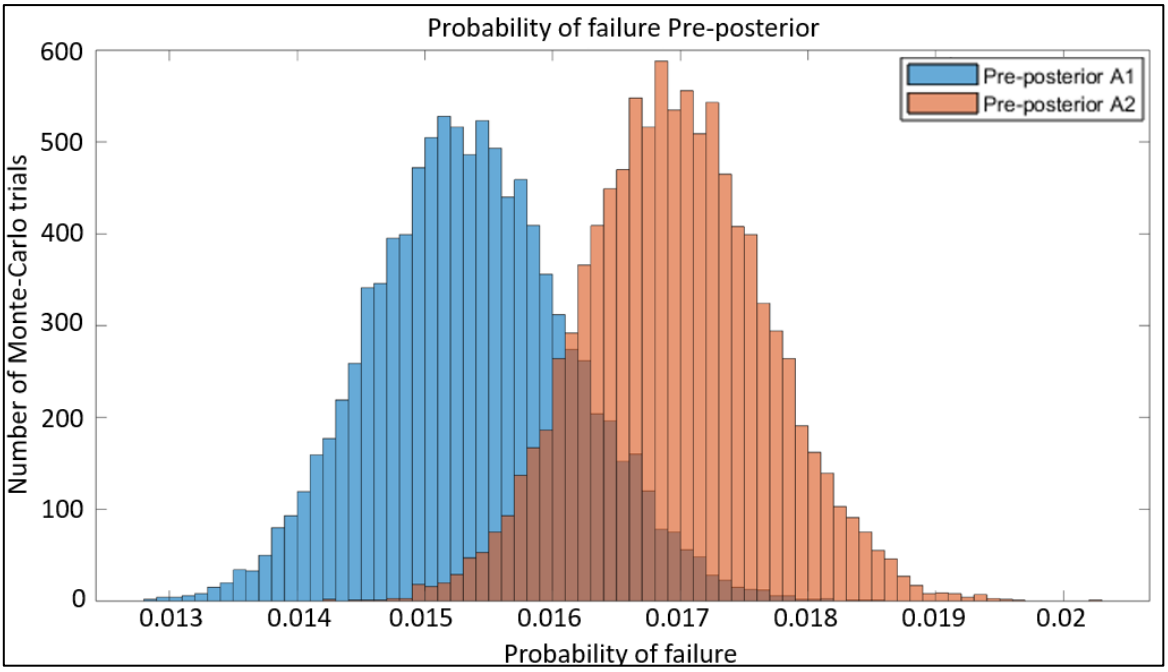

Figure 42: Distributions of probability of failure after Bayesian updating (Pre-posterior), for A1 and A2.

Much like for the prior analysis, the associated distributions were used in Monte Carlo simulation for 10 000 iterations to characterize the resulting costs. The results are shown in Figure 43. The mean pre-posterior cost for A1 was 90.95 millions of SEK and the mean cost for A2 was 94.19 millions of SEK, showing that A1 retains its position as the preferable alternative after the virtual campaign. Since the probability of failure has been drastically reduced after the Bayesian updating, these mean costs are both quite close to the construction cost of each respective alternative.

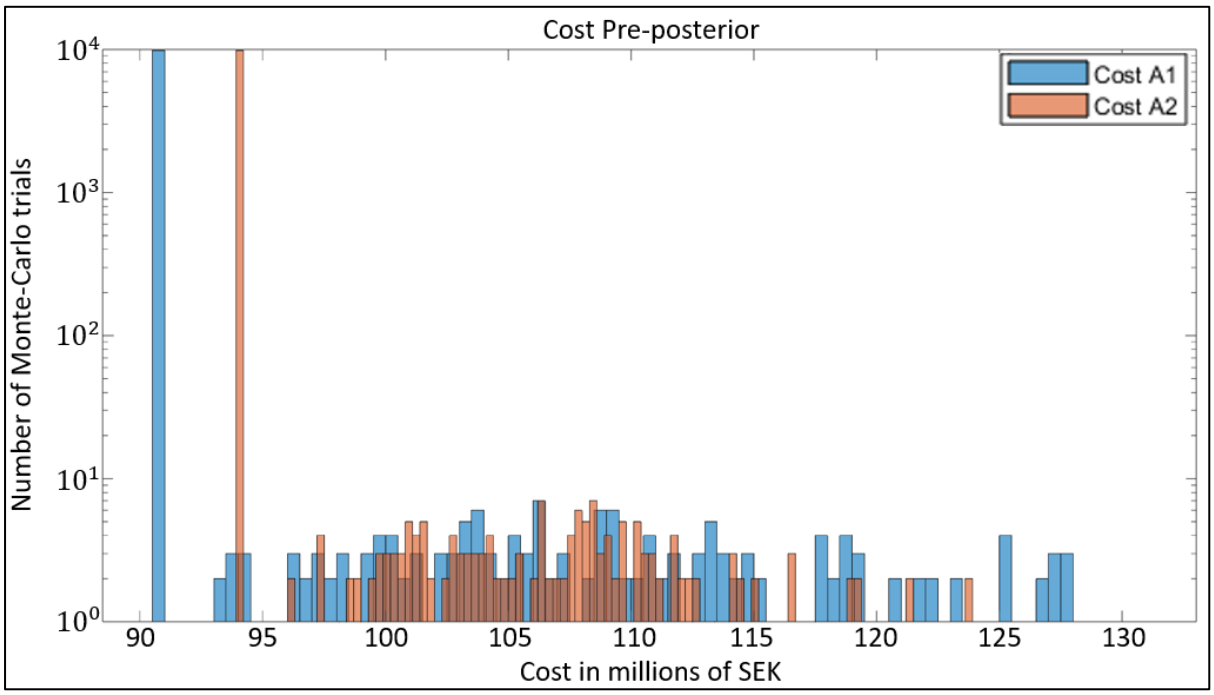

Figure 43: Cost for A1 and A2 in terms of millions of SEK in the pre-posterior analysis.

Given that the alternative A1 performed better in the both the prior and pre-posterior analysis, the campaign would not result in a different decision being made and is therefore not worth conducting

according to the analysis. If it had been worthwhile, the cost of conducting the campaign would be calculated as in equation 7:

$$Total\ cost\ of\ campaign\ in\ SEK = 53\ 000 + A * B * 4550 + A * 64500$$

When performing the analysis, the number of investigations was set to 10 and the depth to 50 meters (5 cells), but 50 meters is not deemed a realistic number for actual drillings. In a real-world case the drillings would be much more likely to be done down to the depth of the tunnel, and since the mean depth of the tunnel is equal to 81 meters this was deemed more reasonable of a value to be used for the purpose of cost calculation of the drilling campaign. As such the total cost of the campaign is:

$$Total\ cost\ of\ campaign = 53\ 000 + 10 * 81 * 4550 + 10 * 64500 = 4.38\ [millions\ of\ SEK]$$

4.3. Sensitivity analysis

Some choices and variables of certain interest have been examined through a sensitivity analysis. Due to time constraints, not all parameters have been included in this, thus focus has been put into the ones created within this specific project (i.e. the threshold value and SCOOB-number). The sensitivity analysis covers:

- The number of SNESIM-simulation iterations performed
- The threshold value for handling issues related to noise
- The SCOOB-number
- Number of core drillings performed in the virtual sampling campaign

Figure 44 presents results in terms of distribution of probability for deformation zones in cells along the tunnel for four different analyses. The difference between the analyses is in the number of SNESIM-simulation iterations performed. As seen in the figure, the intensity of cells with probabilities ranging from 0.2 to 0.6 drastically drops with increasing numbers of iterations. This is most likely since a larger number of iterations tend to even out the noise in the parts of the model uninfluenced by conditioning data. A larger number of iterations also results in more cells having a probability of deformation below 0.2. The analysis performed with 300 iterations does not differ much from the one used throughout this project (200 iterations, illustrated in Figure 34). This implies that a somewhat steady state has been reached. However, to ensure that a steady state is reached, a much larger number of iterations would need to be performed and analysed.

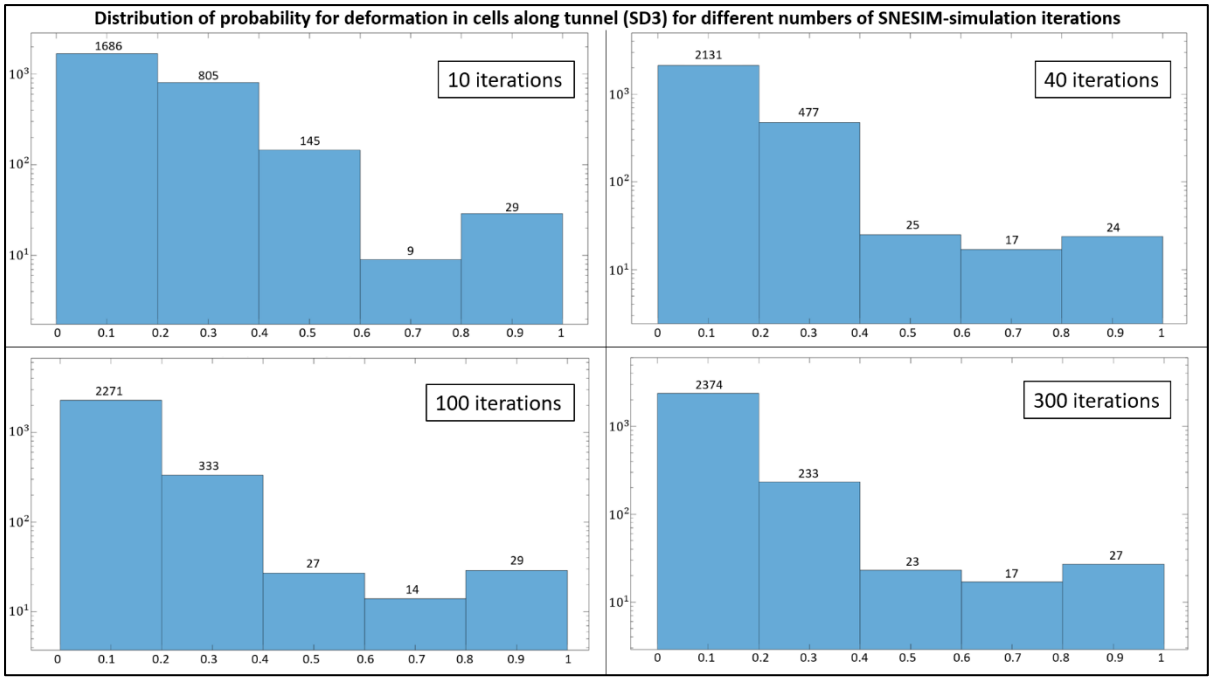

Figure 44: Distribution of probability for deformation in cells along tunnel (SD3) for different numbers of SNESIM-simulation iterations.

The impact of changing the threshold value is illustrated in Figure 45. Raising the threshold value will remove a larger number of cells, including ones with higher probability of deformation. Because of this effect, it is generally observed that a higher threshold value results in lower numbers of deformation zone cells after running the simulation. There is a peak around 23-24 deformation zone cells for analyses performed with the threshold value set to 0 and 0.5*unif(0,1,5) (0.5 times the threshold value selected for the performed analyses, illustrated in Figure 37). This could be explained by the fact that once the threshold value is reduced, SCOOB becomes the determining factor in deciding the number of deformation zone cells. Since the standard definition for SCOOB is unif(0,200) the mean is 100, which seems consistent with the fact that there is a peak around 24 deformation zone cells given that the tunnel has around 2600 cells in total. Furthermore, the number of deformation zone cells is sensitive to both increases and decreases in terms of threshold value.

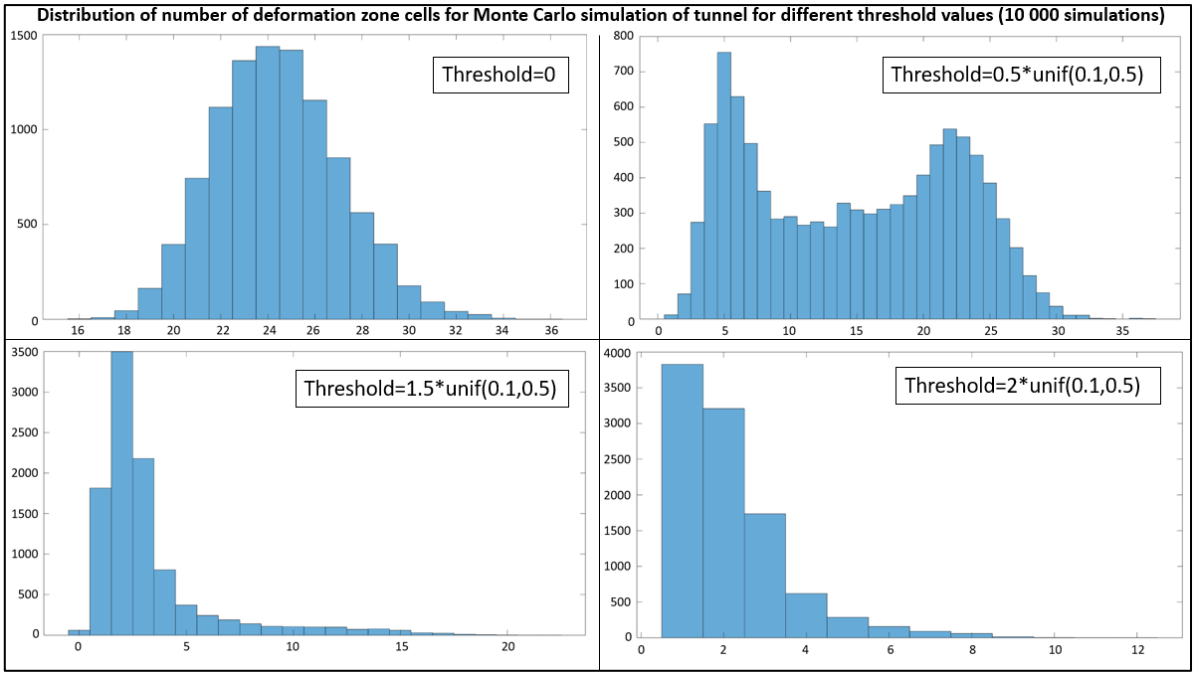

Figure 45: Distribution of number of deformation zone cells for Monte Carlo simulation of tunnel for different threshold values (10 000 simulations).

Figure 46 showcases the sensitivity of the number of deformation zone cells to changes in the definition of the SCOOB distribution. For lower values of SCOOB, the effect is drastic as seen in Table 7, showing a mean of 89.4 deformation zone cells and a mode of 47 for a SCOOB of 0. For higher values of SCOOB however, the impact is much less noticeable. This effect presumably stems from the fact that changes to SCOOB matter much less once they are large enough to account for the clustering effect. Given that the number of deformation zone cells grows drastically at lower values of SCOOB, it can be assumed that the continuity of the deformation zones is of critical importance to the way the analysis is structured as it stands.

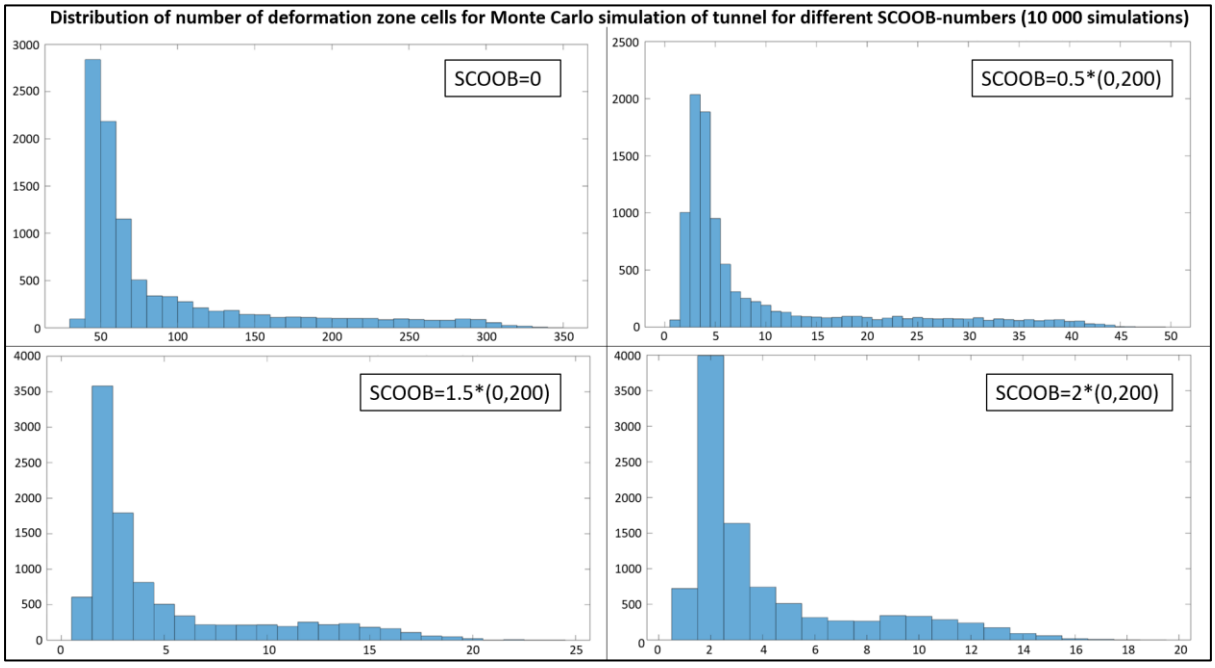

Figure 46: Distribution of number of deformation zone cells for Monte Carlo simulation of tunnel for different SCOOB-numbers (10 000 simulations).

Another topic for sensitivity analyses was the impact of number of core drillings. Figure 47 shows the resulting Beta-distributions from differing numbers of core drillings. As can be seen in Table 8, with an increasing number of core drillings, the probability of failure also decreases. The probability of failure becomes very low with increasing amounts of core drillings, resulting in the construction cost becoming the main factor in calculating the total cost of each alternative. In the extreme case of 100 core drillings, the pre-posterior probability of failure is 0% for both A1 and A2. This stems from the fact that the number of expected deformation zones is never less than 12, resulting in a detection rate of 100%.

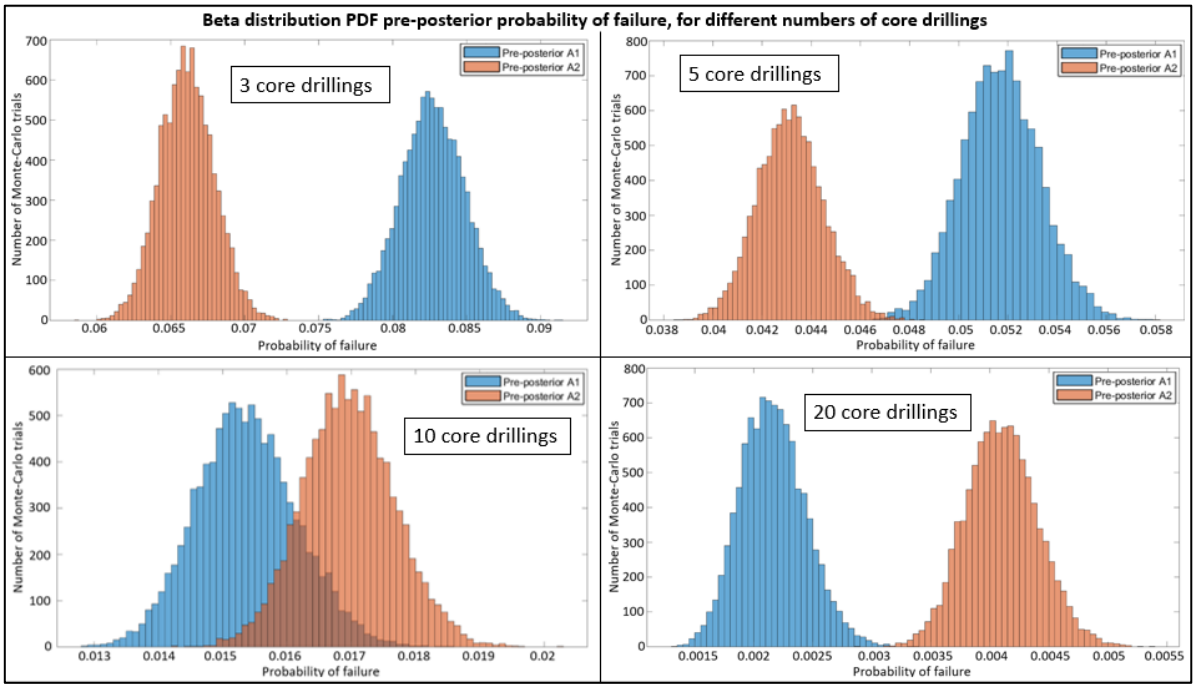

Figure 47: Beta distribution PDF pre-posterior of failure, for different numbers of core drillings.

Table 7: Results of sensitivity analysis for threshold and SCOOB parameters

Adjusted parameter	**Mean number of deformation zone cells**	**Mode number of deformation zone cells**
Standard settings	6.5	2
Threshold=0	24.5	24
Threshold=0.5*unif(0.1 , 0.5)	14.7	5
Threshold=1.5*unif(0.1 , 0.5)	3.3	2
Threshold=2*unif(0.1 , 0.5)	2.16	1
SCOOB=0	89.4	47
SCOOB=0.5*unif(0 , 200)	9.5	3
SCOOB=1.5*unif(0 , 200)	5.0	2
SCOOB=2*unif(0 , 200)	4.2	2

Table 8: Results of sensitivity analysis for number of core drillings conducted

Number of core drillings	Mean pre-posterior cost A1 (millions of SEK)	Expected pre-posterior probability of failure A1	Mean pre-posterior cost A2 (millions of SEK)	Expected pre-posterior probability of failure A2
3 Core drillings	92.15	8.3%	94.92	6.6%
5 Core drillings	91.60	5.2%	94.60	4.3%
10 Core drillings	90.95	1.5%	94.19	1.7%
15 Core drillings	90.8	0.56%	94.10	0.82%
20 Core drillings	90.75	0.21%	94.06	0.41%
100 Core drillings	90.7	0%	94	0%

5. Discussion

In this section, both presented results and alternative approaches are discussed. Furthermore, probable implications associated with different choices are presented. There are many aspects of the project that carry uncertainty, and discussion regarding alternative choices and approaches have been on-going throughout the entire project. While some of these alternative approaches are brought up during discussion, many have also been cut due to lack of relevancy or time constraints. Hence, the ones covered in this discussion section are the ones assumed to be of importance to either the results or future research.

What is important to emphasize is that all analyses are made on the geostatistical model, and not the reality. The geostatistical model is built to estimate how the reality could potentially be interpreted and described at the studied site, but whether the model is a fair representation of the reality is unknown. Hence, the results obtained in the analyses do not necessarily represent what could be expected on-site. Since this study aims to exemplify a methodology rather than constituting decision support for the specific tunnelling project, a potentially poor representation of reality is not considered a problem, nor something reducing the quality of the work performed.

5.1. Geostatistical modelling

The following sections cover topics of discussion regarding important findings and issues that have been encountered during the execution of the methods related to the geostatistical modelling phase, described in section 3.2 Furthermore, this section is divided into two separate parts: “Prerequisites for simulation”, and “Simulation and model construction”. “Prerequisites for simulation” covers discussion topics related to the methods sections 3.2.2 through 3.2.4 (i.e., construction of training images, conditioning data for SNESIM, and definition of simulation grid), and “Simulation and model construction” covers the remaining parts of section 3.2.

5.1.1. Prerequisites for simulation

As described in section 3.2.2, the training image used was constructed based on characteristics (strike, dip, and number) associated with recorded fractures within structure geological domain 3. Information regarding expected fracture density within the rock mass at the site was not considered when constructing the training image, hence the distance between deformation zones in the training image is not based on any specific information. To properly construct a realistic training image, some well-motivated judgement on fracture/deformation zone density would be appropriate (Boucher et al., 2010). This could possibly be achieved through additional communication with experienced geologists in the context of an interview. A well-constructed and realistic training image would have a large positive impact on the final model, in terms of reality representation. To create a model closer to reality, more focus and work would need to be put into the development of the training image.

The way the tunnel depth is handled in SGeMS, using the distance between the tunnel and the ground level (referred to as ΔZ in section 3.2.4) to define the vertical position of the tunnel throughout its geometry, results in slightly incorrect positions of other data (deformation zone simulation results and data associated with performed core drilling tests). As described in section 3.2.4, the reason for defining the tunnel this way is that 3-dimensional simulation grids appear as rectangular blocks in SGeMS. However, defining the ground level as completely flat results in vertical displacements regarding both simulated deformation zones (since the locations underground are

calculated using trigonometric functions) and performed core drilling test results (since vertical placement of these are not defined using ΔZ). Consequently, a line that appears to be straight in the simulation grid would in fact be crooked in reality.

The resolution of the training image and the simulation grid used is set to 10 meters in all three dimensions. This selected resolution is a compromise considering both the increased accuracy of a model with high resolution, and the faster simulation run-time related to a lower resolution. Since the long run-time for the simulations performed has been a limiting factor during the execution of the project, raising the resolution was not an alternative considering the time constraints. Increasing the resolution may possibly be a way to increase the overall quality and accuracy of the model. However, this may possibly result in increased issues regarding some aspects such as the high level of noise, so before considering a higher resolution, a more thoroughly motivated set of parameter settings within the SNESIM algorithm is recommended.

5.1.2. Simulation and model construction

Since all parts of this project are highly affected by the quality of the constructed model, choosing an adequate simulation approach, as well as reasonable values for the associated settings in SGeMS is crucial for the overall quality of the coming analyses (i.e. the CBA and the VOIA). In the case of this study, the researchers had no experience using neither SGeMS nor the selected simulation algorithm, SNESIM. Uncertainties regarding the choices within the simulation part of the model construction are therefore probable to have a large impact on the final model, hence the potential of increasing the accuracy and quality is likely high. Several issues encountered regarding simulation and optimization of the simulation method were handled through large numbers of trial tests, where different variables were changed at a time and effects were recorded. Due to the time constrains within the project, the modelling phase could not have been prolonged. If a similar project is to be done, it is recommended to have some previous knowledge/experiences regarding the SNESIM-algorithm and the SGeMS software. Alternatively assessing different possible simulation approaches through discussion or interview with an experienced SGeMS user. This could have a positive effect both on the time perspective of the modelling phase, and the quality of the final model constructed.

As described in section 3.2.5, all deformation zones defined in the training image was given a width of 3 cells for the purpose of better pattern reconstruction during simulation. As a result of this, the additional deformations simulated on the simulation grid would also have a width of 3 cells. To handle issues related to wide areas of probable deformation zones in the final model, the SCOOB-number was introduced. Using the SCOOB-number to avoid non-representative large amounts of deformation zones requires some reasoning on the SCOOB-number selection. This opens for further sources of error. Ideally, a more thorough optimization of the algorithm settings would result in sufficient pattern reconstruction even if deformation zones would be defined without additional width in the training image. If this was managed, the SCOOB-number setting would perhaps have less impact in coming analyses, due to the higher precision of the final model. In the sensitivity analysis it was made clear that the definition of the SCOOB-number has a major impact on the resulting number of expected deformation zones, and as such, a major impact on the analysis as a whole. Given the impact of the parameter, it is a definite subject for calibration in further work.

The different types of conditioning data (i.e. mapped deformation zones on the surface, and results from core drilling tests) affect the geostatistical simulation results differently. When observing the finalized model, it is obvious that the conditioning data constituting of mapped deformation zones at the surface has a larger impact on the simulation results, than the conditioning data consisting of

core drilling test results. The reason for this is not known, but there are some known differences between the two types that might impact the simulation results. First, the mapped deformation zones at surface are long and continuous lines. This matches the definition of deformation zones in the training image. The core drilling test results only constitute of single points defined as either deformation zone or non-deformation zone. This does not represent the way deformation zones are defined in the training image, and thus may potentially not match with anything in the library of patterns extracted from the training image during simulation. Likewise, the mapped deformation zone data at surface is defined with a width of 3 cells, according to the deformation zone definition in the training image. The single core drilling test result points, representing either deformation zones or non-deformation zones will during simulation only assign information in one cell of the simulation grid. Since there are no deformation zone cells occurring alone in the training image, matching the ones representing core drilling test results to patterns in the training image may be problematic. Applying the same principle here as in the training image and using multiple deformation zone cells as for the purposes of defining the conditioning data might as such be preferable to using singular points.

An alternative to creating one probability-based model- constituting of several geostatistical simulation realization, used for the CBA and VOIA analyses- would be to perform the whole chain of tasks (illustrated in Figure 9) for each of the geostatistical simulation realizations performed. In this case, it would result in 200 binary geostatistical models, followed by 200 CBA and VOIA analyses. All results gathered would then be analysed statistically by establishing distributions on the aspects of particular interest. The reason for not using this approach was the high prevalence of singular deformation zone cells disconnected from the larger networks showing up in the realizations- regarded as noise. Using each realization individually, these individual deformation zone cells would be handled equally as the ones clearly influenced by conditioning data and ones consistently appearing in broader patterns- leading to potentially misleading results. In the probability-based model, all deformation zones not influenced by the conditioning data appear as background noise in terms of unrealistic high continuous levels of deformation probabilities throughout the whole model. The deformation zones interpreted as noise would thereby be separated from the ones influenced by conditioning data through differing magnitudes of probability. This separation is handled by introducing the threshold described in section 3.3.3. A threshold could not have been implemented this way if the alternative approach, i.e. performing the whole chain of tasks on all realizations, was to be used. It is possible, or even probable, that the alternative method would have been implemented, in case the simulations did not display this large amount of noise.

A noteworthy discovery regarding the simulation results in SGeMS is that cells outside of the simulated simulation region have been influenced by conditioning data. As a result of this, cells outside of the simulated region have been given values even though they should not (1 or 0/deformation or non-deformation). This was discovered during data analysis and handling in MATLAB and was fixed quickly. However, this was a surprising discovery that could have led to probable negative implications if it had not been addressed.

5.2. Value of information analysis

Given the time-constraints, the VOIA conducted in this project was of narrow scope, with most, if not all of its integral parts being possible to expand upon given a broader timeframe and room for further research.

5.2.1. Cost-benefit analysis

The cost-benefit analysis framework to start with, is the cornerstone of the analysis. In this project, only two alternatives are evaluated (A1 and A2). Given that the difference in mean cost between the prior and pre-posterior for A1 is 93.48-90.95 = 2.53 [millions of SEK] it is possible that a differently framed alternative A2 would result in a different alternative having a lower cost after the investigation, making it worth conducting. Given that the probability of failure was drastically reduced after the Bayesian updating an alternative preparing for less deformation zones would most likely be the superior alternative in this context, as the construction cost largely becomes the deciding factor.

A pre-posterior probability being this low is of course a matter of feasibility. In another setting, these alternatives could be expanded upon to give further insight into to what extent it is worth preparing for deformation zones beyond what is expected based on engineering geological prognoses. In this project, the more conservative alternative A2 which accounts for uncertainty in the prognosis by preparing for twelve deformation zones in SD3 instead of seven could be expanded on further given the simple framework established, to also determine which number of deformation zones is best to account for given the uncertainty of the model.

Another important factor related to the CBA are the costs related to the alternatives. There are two types of costs considered in this project- the costs related to construction of the two alternatives, and those related to failure. The construction cost to start of with is also subject of heavy simplification in the project and has been defined only by the difference in amount of higher class grouting between alternatives, with these numbers being based on those from the Varberg tunnel project. While it is a heavy simplification to only use the cost of grouting measures as a so-called construction cost, it can be viewed as suitable to the project. Naturally any tunnel project would include a large amount of different costs outside of the grouting, but since this analysis is only interested in a comparison between alternatives, only the costs that differ would be of interest to the analysis. Since the only difference between alternatives A1 and A2 is the extent of which higher class grouting measures are used, it is reasonable to only consider these costs when conducting analysis. The same argument was in this project used for the exclusion of benefits from the objective function since the benefit would also be equal between alternatives (a working tunnel).

The costs of failure, however, is something that could very well be expanded on. In this project, the cost of failure was characterized by two modes of failure- encountering an unexpected (water bearing) deformation zone and encountering low quality rock such that reinforcing measures would be required. Both modes of failure result in a delay of a number of days, and the cost of failure is seen as dependent on the number of days that the project is delayed. During the actual construction phase, these costs will exhibit much more nuance than what could be accounted for in this project. First, the extent as to how many days of delay any unexpected deformation zone could cause is entirely up to the scale and nature of the deformation zone. A single deformation zone that is small or clay filled could very well be ignored given that leakage requirements are often framed as litres per minute per 100 meters of tunnel, but a larger deformation or multiple reoccurring ones could require extensive measures. The characterization of costs of failure was done through expert elicitation of an expert with experience of a similar tunnel project that ran into issues with unexpected deformation zones. To account for uncertainty, an elicitation strategy was applied where the objective was to establish distributions of possible values instead of deterministic quantities. One way of getting more nuance in the characterization of failure within this project would be to conduct more interviews or include a larger number of experts to gain further input.

5.2.2. Probability of failure

The definition of probability of failure has been a frequent topic of discussion in this project. In the finalized methodology described in this report, the probability of failure has been defined as a beta-distribution with its related alpha value representing the number of iterations of a Monte Carlo simulation where more than the expected value of deformation zones was encountered, and the beta value representing the number of iterations of a Monte Carlo simulation where this value was not exceeded. This method of defining the probability of failure has several advantages:

- Using a distribution rather than a fraction allows for uncertainty to be considered.
- A beta-distribution allows for simple Bayesian updating.

Hence, the probability of failure was defined in this way largely to enable the Bayesian updating. While using a beta-distribution to describe uncertainty in a probability like this does not pose an issue, the definition of the related alpha and beta parameters as the number of iterations of a Monte Carlo simulation exceeding/not exceeding the expected number of deformation zones does create an issue. Since the variance present in the results of the Monte Carlo simulation in regard to number of deformation zones is not accounted for in the beta-distributions, and since the spread of the distribution decreases with an increasing amount of Monte Carlo trials, the uncertainty presented is misrepresented. This effect is best seen in Figure 36-Figure 37, where the variance seen in the number of deformation zones of different simulation results in Figure 40 is not represented as uncertainty in the beta-distribution of Figure 38 and Figure 39. As such, a way to define the beta-distribution considering the variance is warranted. One way to account for this would be to define the alpha and beta parameters according to equation 8:

$$\alpha = \left(\frac{1-\mu}{\sigma^2} - \frac{1}{\mu}\right) * \mu^2,\ \beta = \alpha * (\frac{1}{\mu} - 1) \qquad (8)$$

Given that the mean and variance of a beta-distribution can be defined as in equation 9 (Clyde et al., 2022):

$$\mu = \frac{\alpha}{\alpha+\beta},\ \sigma^2 = \frac{\alpha\beta}{(\alpha+\beta)^2(\alpha+\beta+1)} \qquad (9)$$

where mu is the mean value and sigma the standard deviation. While this alternative approach of defining the beta-distribution would address not only the misrepresentation of variance in the model, but it would also fix the issue of increasing amounts of Monte Carlo trials leading to a tighter distribution. The reason for not proceeding with this alternative approach was that there was no clear way of representing the standard deviation through the data. While the mean value could be naturally defined as a fraction of trials exceeding the expected number of deformation zones, defining the standard deviation proved troublesome. In theory, this standard deviation would in some manner reflect the variance seen in the distribution of number of deformation zones in the Monte Carlo simulation in Figure 37. However, no way of expressing this variance in the form of a Bernoulli-trial of exceeding a certain amount of deformation zones was uncovered in this project- and could therefore be the subject of further research on the topic.

Another subject of discussion related to the calculation of probability of failure was the implementation of the SCOOB-number and threshold value distributions, where the SCOOB-number was implemented to address continuity of deformation zone probabilities in the geostatistical model and the threshold value was implemented to address noise. Both measures were introduced as means of covering for lacking quality in the model. As mentioned in 5.1, it was decided in the project that instead of looking at singular model results from the SNESIM algorithm for purposes of analysis, all the individual results would be compiled into a single probability-based model where the value of

each cell corresponds to the mean of all simulations. The reason for doing so was that the resulting output of single model simulations included a lot of noise- noise in the sense that there were a lot of individual deformation zone cells outside of the expected patterns. Hence, a measure for addressing this noise had to be introduced, and this was done in the form of a threshold value of probability, where values below the threshold would be nulled. Another issue that had to be addressed was the fact that deformation zones are continuous in nature, and that counting one group of continuous cells as distinct deformation zones would also present inflated numbers of encountered deformation zones. This problem was further worsened not only by the fact that the deformation zones were defined as multiple cells thick in the training images to help pattern recognition, but also because all simulations were compiled to address noise. The result was that deformation zones in the final model were represented by large fields of increased probability of deformation zones. The SCOOB-number serves to address this issue of continuity and could also be argued to account for the fact that injection measures are also by nature not isolated to a single spot but could serve to grout multiple deformation zones if they are close to each other.

Both the SCOOB and threshold distributions serve important functions for the purposes of analysis in this project. They are however defined as distributions, with somewhat arbitrary values as boundaries. There is no clear right or wrong when defining the distributions for these two parameters. Since both distributions have a large impact on the results of the analysis, due precaution was taken to avoid confirmation bias and ensure that they would not be designed in way to produce results that were already expected to occur. This was done by defining them based on what was deemed reasonable values given the function they serve, while also leaving room for representing parameter uncertainty.

Once again, it is important to note that both SCOOB and the threshold value were introduced to address issues caused by the lack of quality in the model. If a geostatistical model of higher quality could be constructed, neither of these parameters would need to be used and hence the issue of making all these decisions on reasonable values while also remaining unbiased could be avoided.

Yet another point of discussion regarding the definition of probability of failure is the very basic structure of how the calculation of number of encountered deformation zones is done for every simulation result of the Monte Carlo analysis. Currently, the method consists of checking the tunnel cell by cell for the probability of deformation. Each cell corresponds to a volume of 10x10x10 meters, and the tunnel consists of 2674 cells in total. If a cell results in a deformation zones, a number of the following cells are skipped for the count in order to account for continuity. While this approach is efficient in its simplicity, it leaves a lot of room for potential adjustments and alternative designs. One clear issue with this approach is that there is no distinction made between singular cells resulting in a deformation zone and large clusters of cells with high probability of deformation zones. As noted in the discussion of the CBA, the model as it stands misses out on a lot of potential nuances in terms of characterizing costs. A deciding factor when it comes to the extent of how expensive an unexpected deformation zone could be is its scale. While a smaller deformation zone might not need to be addressed, larger ones could require extensive additional grouting or even reinforcement if the rock quality is deemed insufficient. If the geostatistical model is implying that a chunk of the tunnel poses high probability of deformation zone, this could well be used as input for deciding on the scale of the cost of failure as well.

Furthermore, this strategy of looking at larger sets of cells could also be used as an alternative method to check the tunnel for deformation zones cell by cell. Since one injection shield covers a large volume of rock, the corresponding volumes worth of cells could instead be analysed for the presence of deformation zones. Based on the presence of deformation zones in this volume, a

choice of grouting method can be decided upon, and the cost of failure could depend on the amount of deformation zone cells for a particular segment. This kind of measure could also work as a way of opening up to include even more nuance in the model, as different types of deformation zone cells corresponding to different rock qualities or could be included as different categories in the geostatistical model. Another potential adaptation that could be done within this framework is to conduct the virtual core drillings in these chunks instead of on the surface, which would mirror the methodology used by Zetterlund et al. (2011) and could potentially be a more suitable means of Bayesian updating than the methodology presented in this project.

5.2.3. Bayesian updating

The design of the virtual core drilling campaign was another part of the methodology created from the ground up for the purposes of this project. In similar analyses such as those exemplified by Freeze et al. (1992) and Zetterlund et al. (2011), the gathering of virtual information was done binomially, addressing the issue of a highly permeable layer existing or not existing in the case of Freeze et al. (1992) or a virtual drilling either encountering or not encountering a deformation zone in the case of Zetterlund et al. (2011) In the context of this project however, the investigated outcome is not strictly binomial per se, since the amount of deformation zones also impacts the cost. While it is true that the question of if a certain amount of deformation zones is exceeded or not is binomial, what is of interest to the campaign is also to gain further insight into what number of deformation zones is expected to be encountered in the tunnel under construction. Moving from making assertions on the number of expected deformation zone cells given virtual data collection by looking at a limited number of cells was seen as best solved by looking at the mean probability of deformation zone found in the campaign and applying this probability to the total number of cells in the tunnel for analysis. Thereby an assumption is made that the rate of occurrence of deformation zones behaves stationarily in the rock, that is if a total of seven deformation zones was expected to appear in a volume of rock, then seventy would be found in a rock volume ten times bigger. While there is logic to this approach of conducting the virtual campaign, it does present several potential issues.

First, the idea of applying a mean probability of deformation zone over a larger number of cells is highly theoretical and far removed from reality. Spatial continuity of deformation zones is not represented at all this way and the actual geographical location and placement of deformation zones are not considered at all. Furthermore, there is also the issue of keeping consistency with the application of the SCOOB and threshold of probability from the calculation of the prior probability of failure. In order to remain consistent, the very same distributions for SCOOB and threshold of probability has been applied when calculating the number of deformation zones encountered using the mean probability. It is unclear whether this approach of using the same distributions is reasonable. For example, given that the lower limit of the threshold of probability distribution was set to 0.1 to reflect the mode of all cells in SD3, it might be reasonable to instead use the mode value of all cells in the upper five cells of the model surface since this is where the virtual campaign was conducted. Since the mode value for the surface cells is higher, this would have meant that the expected value of the threshold distribution would be higher and hence the number of deformation zone cells encountered in total would be lower. This result could be seen as more reasonable as the increase in probability between the prior and pre-posterior is drastic, but handpicking methodology to get results closer to what was expected is biased and not scientifically amenable, hence the distributions were kept consistent between prior calculation of probability of failure and the campaign.

Other aspects of consideration are the distribution and geometry of the virtual core drillings. In the project this was kept simplified, only resorting to vertical cores randomly distributed on the surface above the tunnel. Since the quality of the model deteriorates with depth, they were also limited to five cells (or 50 meters) of depth. When performing real core drillings, they are often executed at strategical angles or even directed straight through the tunnel to collect as much valuable information as possible (Spinos, 2024). Furthermore, investigation campaigns can be designed with search theory in mind, to take into consideration the probability of finding a certain geometry given a specific search grid (Savinskii, 1965). These considerations were however considered out of the scope of the analysis. Especially given that the detail level of the model is low, and that the quality of the model is considered higher close to surface compared to the depth of the actual tunnel. Yet another aspect worth noting is that typically, core drilling investigations are done in spots where deformation zones are expected to occur. This sort of campaign where the placements of core drilling investigations are randomly distributed on the surface gives an inherently different type of input information than what would normally be procured. Having better understanding of not only the presence of deformation zones, but also higher quality rock in the area could potentially give decision support in other areas as well. Taking account the effects of the diminishing returns of the value of information provided by performing additional core drillings that could be observed in the sensitivity analysis are also of interest for further studies.

In regards to the results of the updating themselves, it is noteworthy that there is a significant decrease in probability of failure between the prior and pre-posterior. It is clear from the results that the expected number of deformation zones is higher near the surface than deeper in the model, as can be understood given that the probability of failure decreases with more core drillings being made in the sensitivity analysis. While an assumption is made in the context of this project that the surface of the model is of higher quality as it is impacted more by the conditioning data- it is in reality impossible to confirm whether the calculated distributions of encountered deformation zones is more accurate in the prior or the pre-posterior without proceeding with the actual excavation of the tunnel. As such, validating and updating the model to better fit with the actual sightings during the excavation of tunnel would be essential in improving the general methodology as a whole. This could serve as a means of both adjusting the geostatistical model and the parameters used in the VOIA segment.

5.2.4. Value of information analysis

Based on the calculated prior and pre-posterior costs and the cost of the campaign it could be concluded that the core drilling campaign is not worth doing. However, while there was a clear difference in prior costs for the two alternatives, the pre-posterior costs became highly dependent on the construction cost given the low probability of failure. As earlier noted, given that the construction cost was the determining factor between the alternatives, a less conservative alternative would likely perform better than the reference alternative A1.

In addition, it is worth noting that the scope of which the value of information is taken into consideration within this sort of analysis is highly limited. In reality, a core drilling campaign could also be of value within other fields of study or for further decision support done by experts. Examples of such instances where the information from core drillings are of use include the characterization of the hydrogeology or rock quality of the site (Monicard, 1980).

5.3. Future research

Given the broad scope of this project there are several topics of interest for future research.

5.3.1. Geostatistical modelling

Since only SD3 have been fully modelled, this study lacks methods to handle the differences between structural domains during simulation, and potential related issues. Including SD1 and SD2 in the model construction would imply the need to consider the boundaries between domains. This could proposedly be done through implementation of so called “Soft data” in SGeMS. Soft data refers to data associated with probabilities (Y. Liu, 2006), unlike the hard data used as conditioning data in within this project. The results of the 200 iterations performed on SD3 could in that case be exported from SGeMS, summed up, and imported again as soft data. The soft data regarding SD3 would then be included as conditioning data when simulating on SD2, to hopefully achieve continuity at the boundary. The same procedure would be repeated for the boundary between SD2 and SD1. Trial tests performed showed potential in this method, but further research would need to be done for the purpose of optimizing and examining this methodology.

One of the limitations stated in section 1.1 is that the rock mass is divided into two separate categories during model construction: 1) “bulk rock” and 2) “permeable deformation zones”. This is a major simplification, that presumably implies limitations regarding reality representation of the final model. For this study, additional categories relating to less permeable entities within the rock mass, such as clay filled deformation zones or smaller fractures, could be interesting to implement. This is furthered motivated by the fact that inadequate rock quality (which relates to deformation zones, regardless occurrence of filling material in the fractures) is interpreted as a potential cost. Including additional categories within the geostatistical model could be a way to account for the large complexity associated with rock masses. Investigating and potentially implementing additional categories during model construction and following analyses is therefore recommended for future research.

According to Pejman (2018), pattern based multiple point statistics methods would theoretically perform better than pixel-based methods in reconstructing large, complex structures. In SGeMS however, FILTERSIM and SNESIM are the only MPS algorithms of choice, where the pattern based FILTERSIM only should be used in case of 4 or more categories or continuous variables are in use, according to the SGeMS manual (Remy et al., 2009). Thereby, it would be of interest to examine other MPS algorithms, potentially outside SGeMS.

An alternative and possibly better way to handle the fact that simulation grids in SGeMS appear as rectangular blocks could be to divide the simulation grid region representing SD3 into two separate regions. One representing the area constituting of rock mass and the other representing the soil/air above. If the boundary between these regions is shaped as the top of the rock mass, simulating on the bottom one would generate results only within the rock mass, with geometrically continuous results at depths (i.e. non-crooked dips). If this method was to be used, the conditioning data based on mapped deformation zones on the surface would need to be projected onto the region boundary. Using a general reference coordinate system for both the simulation grid and all conditioning data would in this case result in all geographically defined data (i.e. core drilling results and mapped deformation zones) being correctly located in the simulation grid.

5.3.2. Value of information analysis

As noted in earlier discussion, it is important to note that the methodology exemplified in this project regarding application of value of information analysis has had its design heavily influenced by the quality of the geostatistical model- with the two introduced parameters of the SCOOB-number

and the threshold value possibly having alternative options of implementation to address their corresponding issues. SCOOB for example, has in the context of the project been defined with the clustering of higher probabilities of deformation zone present in the data in mind, whereas an idealized model of high performance and resolution could instead consider the orientation of deformation zones and their adjacency. Taking better consideration to the spatial aspect in particular would be of interest since grouting is by nature not isolated to a single point but is spread out in a shield through the rock. Addressing the issue of noise could also be done differently for a model of higher quality. In the project, it was done practically by saying that any cell in the model that did not have a deformation zone in a certain fraction of the total simulations. An example of different alternative could be to implement a continuity requirement, where any deformation zone cell not being part of a large enough set of cells would be considered noise. These are just some examples of ways of addressing continuity and noise however, any real measures would have to be designed with the actual model in mind- taking factors like resolution and presence of different categories in mind.

Another key topic of interest for further research is the general methodology behind both the evaluation of number of deformation zones encountered and the virtual core drilling campaign. As brought up in earlier discussion, calculating the number of deformation zones by analysing the tunnel cell by cell is a simple way to go about it, but if more nuance was to be implemented into the model through more categories than simply deformation zone/ non-deformation zone then a different method would have to be developed. As for the probability of failure, the methodology exemplified in this project was designed in a way to allow for simple Bayesian updating using beta-distributions related to the number of expected deformation zones being exceeded or not. This was largely to allow for Bayesian updating to be done in a simple manner but should ideally be developed to better include variance and uncertainty. The Bayesian updating itself also requires more development, especially since the virtual core drilling campaign is highly simplified. Based on the design of the campaign, the probability of encountering a certain geometry could also potentially be determined using search theory (Savinskii, 1965). Outside of the virtual campaign itself, the means of performing Bayesian updating is another topic for consideration. The methodology presented in this project lacks fundamental connection to geology and only results in an expected number of deformation zones. Developing a method that makes better usage of the information of virtual core drillings could make for meaningful improvement for the framework as a whole.

The value of information as defined in this project is also limited in scope. Ideally this information too should be taken into account for analysis, as it does possess value. One way to take this value into account could be to also check if similar investigations would be done elsewhere in the confines of the project but for different purposes whereafter the cost of conducting those investigations would be added to the value of information of performing them. This method of taking value into account from outside of the boundaries of the analysis would be analogous to system expansion in a life cycle assessment (LCA) context which is a method used to take into consideration the value of byproducts for different processes (Finnveden et al., 2009).

6. Conclusion

The project aims to exemplify a methodology for utilizing multiple point statistics (MPS) and value of information analysis (VOIA) in order to provide further decision support for grouting design in a tunnelling project. This has been done through a case study of Kolmårdstunneln in Sweden, using the MPS-algorithm SNESIM and VOIA of two different grouting designs.

Given the aims of the project, the related conclusions are as listed:

- A methodology of applying MPS-algorithms in the SGeMS software for modelling of deformation zones in crystalline rock mass has been developed through literature studies and trial tests. This resulted in a model with good pattern reconstruction in the horizontal plane, but not as distinct reconstruction in the vertical plane.
- Several geological model realizations have been made using the SNESIM-algorithm. These were combined to create a probability-based model. The individual realizations as well as the probability-based model include a lot of noise.
- The costs of making an erroneous interpretation of the number of permeable water-bearing deformation zones along the tunnel stretch has been quantified through expert elicitation. This resulted in distributions for cost associated parameters, where the main contributor to the cost is the added time required for additional grouting.
- The number of deformation zones encountered in the tunnel geometry has been quantified by analysing the cells of the constructed probability-based geostatistical model corresponding to the tunnel. The developed methodology makes use of Monte Carlo-simulations to establish probability density distributions regarding number of deformation zones encountered. To handle issues related to shortcomings in the model, the threshold value and the SCOOB-number was introduced.
- The methodology developed for conducting the virtual core drilling campaign could successfully be used to perform Bayesian updating. The virtual core drillings were conducted close to the surface of the probability-based model to avoid issues regarding model uncertainty at greater depths.
- The cost of collecting additional data by performing core drillings was quantified through communication with experts. The information gathered was used to estimate the theoretical cost of performing the virtual sampling campaign.
- The economic value of information from further core drilling investigations was evaluated by comparing the prior and pre-posterior analyses for the two grouting designs considered. The results imply that conducting a campaign would not result in a different decision being made, hence it would not be worth conducting for this case study.

In addition to these conclusions related to the aims, multiple topics that should be subject to further research have been proposed in the discussion segment of the project. Some of the topics of foremost importance are:

- Further work in establishing a geostatistical model of high quality. Especially important factors in this regard is the development of training images and a set of parameter settings that are able to capture the complex patterns of fracture networks in both the horizontal and vertical plane. The inclusion of other categories outside of simply bulk rock and deformation zone could also be of interest to add further nuance to the model.
- Increasing complexity in the value of information analysis. This includes evaluation of additional alternatives, defining probability of failure in such a way that uncertainty is better included, development of a virtual campaign more representative of what would be done in

reality, and finally, expanding the concept of value of information to also include benefits outside of the characterization of deformation zones.

- Finally, once the tunnelling project has advanced, new information should be used to validate the results in the presented methodology. Real information regarding the presence of deformation zones could also be used to calibrate and adapt the methodology to better represent the real situation in the tunnel.

References

Aven, Terje. (2003). *Foundations of risk analysis : a knowledge and decision-oriented perspective*. Wiley.

Boucher, A., Gupta, R., Caers, J., & Satija, A. (2010). *Tetris: a training image generator for SGeMS*. http://www.gnu.org/copyleft/gpl.html

Clyde, M., Cetinkaya-Rundel, M., Rundel, C., Banks, D., Chai, C., & Huang, L. (2022). *An Introduction to Bayesian Thinking- A Companion to the Statistics with R Course* (1st ed., Vol. 1). Coursera.

Davis, J. C., Wiley, J., & New York Clxchester Brisbane Toronto Singapore, S. (2002). *Statistics and Data Analysis Third Edition*.

Finnveden, G., Hauschild, M. Z., Ekvall, T., Guinée, J., Heijungs, R., Hellweg, S., Koehler, A., Pennington, D., & Suh, S. (2009). Recent developments in Life Cycle Assessment. *Journal of Environmental Management*, *91*(1), 1–21. https://doi.org/10.1016/J.JENVMAN.2009.06.018

Freeze, R. A., James, B., Massmann, J., Sperling, T., & Smith, L. (1992). Hydrogeological Decision Analysis: 4. The Concept of Data Worth and Its Use in the Development of Site Investigation Strategies. *Groundwater*, *30*(4), 574–588. https://doi.org/10.1111/j.1745-6584.1992.tb01534.x

Grøv, E., & Woldmo, O. (2012). *Modern Pre-Grouting Technology in Norway*. https://doi.org/10.1061/9780784412350.0064

Guardiano, F. B., & Srivastava, R. M. (1993). Multivariate Geostatistics: Beyond Bivariate Moments. *Geostatistics Troia '92. Vol. 1*, 133–144. https://doi.org/10.1007/978-94-011-1739-5_12

Johansson, P.-O., & Kriström, B. (2015). Cost-Benefit Analysis for Project Appraisal. In *Cost-Benefit Analysis for Project Appraisal*. Cambridge University Press. https://doi.org/10.1017/CBO9781316392751

Keisler, J. M., Collier, Z. A., Chu, E., Sinatra, N., & Linkov, I. (2014). Value of information analysis: The state of application. *Environment Systems and Decisions*, *34*(1), 3–23. https://doi.org/10.1007/S10669-013-9439-4/TABLES/4

Liu, X., Zhang, C., Liu, Q., & Birkholzer, J. (2009). Multiple-point statistical prediction on fracture networks at Yucca Mountain. *Environmental Geology*, *57*(6), 1361–1370. https://doi.org/10.1007/s00254-008-1623-3

Liu, Y. (2006). Using the Snesim program for multiple-point statistical simulation. *Computers and Geosciences*, *32*(10), 1544–1563. https://doi.org/10.1016/j.cageo.2006.02.008

Monicard, R. P. (1980). *Properties of reservoir rocks : core analysis*. Éditions Technip.

O'Hagan, A. (2019). Expert Knowledge Elicitation: Subjective but Scientific. *The American Statistician*, *73*(sup1), 69–81. https://doi.org/10.1080/00031305.2018.1518265

Remy, N., Boucher, A., Wu, J., & Srivastava, M. (2009). Nicolas Remy, Alexandre Boucher and Jianbing Wu: Applied Geostatistics with SGeMS: A User's Guide. *Mathematical Geosciences 2009 41:3*, *41*(3), 353–356. https://doi.org/10.1007/S11004-009-9217-5

Savinskii, I. D. (1965). Probability Tables for Locating Elliptical Underground Masses with a Rectangular Grid. In *Probability Tables for Locating Elliptical Underground Masses with a Rectangular Grid*. Springer US. https://doi.org/10.1007/978-1-4684-9027-5

Seeburger, D. A., & Zoback, M. D. (1982). The distribution of natural fractures and joints at depth in crystalline rock. *Journal of Geophysical Research: Solid Earth*, *87*(B7), 5517–5534. https://doi.org/10.1029/JB087IB07P05517

Spinos, K. (2024, May 2). *Personal communication*.

Strebelle, S. (2002). Conditional simulation of complex geological structures using multiple-point statistics. *Mathematical Geology*, *34*(1), 1–21. https://doi.org/10.1023/A:1014009426274/METRICS

Strebelle, & Journel. (2001). Reservoir Modeling Using Multiple-Point Statistics. *Proceedings - SPE Annual Technical Conference and Exhibition*, 97–107. https://doi.org/10.2118/71324-MS

Sweco. (2021). *Injection Concept Stavsjö-Loddby, Ostlänken*.

Tahmasebi, P. (2018). Multiple point statistics: A review. In *Handbook of Mathematical Geosciences: Fifty Years of IAMG* (pp. 613–643). Springer International Publishing. https://doi.org/10.1007/978-3-319-78999-6_30

Trafikverket. (2021a). *Ingenjörsgeologisk prognos*.

Trafikverket. (2021b). *Markteknisk undersökningsrapport, Bergtekniska undersökningar*.

Trafikverket. (2021c). *PM Beräkningar*.

Trafikverket. (2021d). *Tekniskt PM Berg*.

Trafikverket. (2024). *INITIAL HYDROGEOLOGISK SYSTEMBESKRIVNING*.

Vipond, T. (2024). *What is Sensitivity Analysis?* https://corporatefinanceinstitute.com/resources/financial-modeling/what-is-sensitivity-analysis/

Zetterlund, M., Norberg, T., Ericsson, L. O., & Rosén, L. (2011). Framework for Value of Information Analysis in Rock Mass Characterization for Grouting Purposes. *Journal of Construction Engineering and Management*, *137*(7), 486–497. https://doi.org/10.1061/(asce)co.1943-7862.0000265

Appendix

Appendix 1: Pole density diagram including interpreted crack groups within structure domain 1. The green line refers to main tunnel directions (70°-250°).

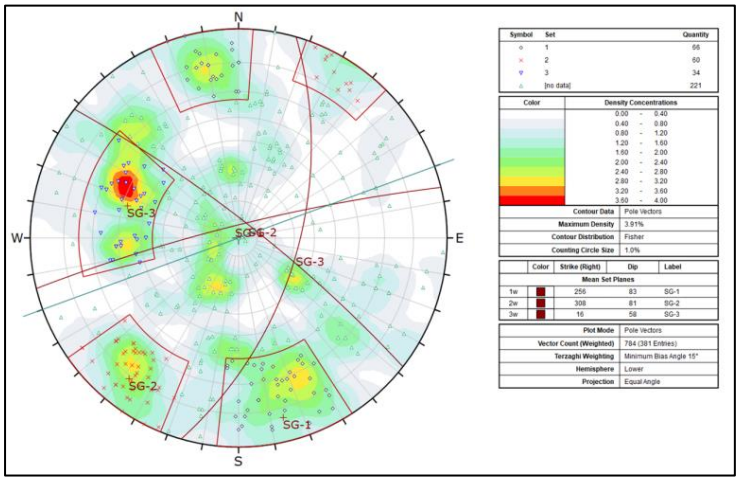

Appendix 2: Orientation of interpreted crack groups within structure domain 1.

Sprickgrupp	Strykning° (variation)	Stupning° (variation)	Sprickor (antal)
SG-1	255±20	85±15	66
SG-2	310±20	80±10	60
SG-3	015±30	60±15	34
Slumpmässiga sprickor			221

Appendix 3: Pole density diagram including interpreted crack groups within structure domain 2. The green line refers to main tunnel directions (70°-250°).

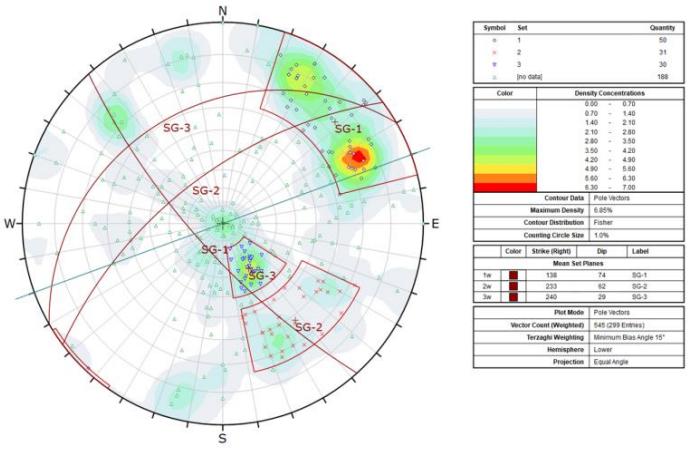

Appendix 4: Orientation of interpreted crack groups within structure domain 2.

Sprickgrupp	Strykning° (variation)	Stupning° (variation)	Sprickor (antal)
SG-1	140±30	75±15	50
SG-2	235±25	65±15	32
SG-3	240±25	30±15	30
Slumpmässiga sprickor			187

Appendix 5: Pole density diagram including interpreted crack groups within structure domain 3. The green line refers to main tunnel directions (approximately 60°-240°).

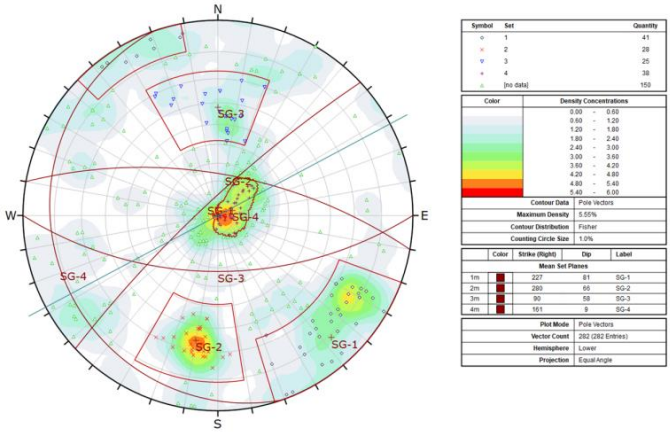

Appendix 6: Orientation of interpreted crack groups within structure domain 3.

Sprickgrupp	Strykning° (variation)	Stupning° (variation)	Sprickor (antal)
SG-1	230±25	80±10	41
SG-2	280±20	65±15	28
SG-3	090±25	60±15	25
SG-4	160±90	10±15	38
Slumpmässiga sprickor			150

Appendix 7: Part of the attribute table including core drilling test results. Column "i" represents occurrence of deformations/cracks.

	x	y	z	i	id
1	572294.150	6504290.705	86.010	0	1
2	572299.489	6504306.212	73.380	1	1
3	572302.419	6504314.721	66.480	1	1
4	572332.974	6504403.458	-5.411	0	1
5	571413.108	6504655.524	89.740	0	2
6	571392.090	6504547.398	2.879	0	2
7	570670.219	6504071.089	47.610	0	3
8	570717.969	6504153.794	7.250	1	3
9	570720.619	6504158.384	5.010	0	3
10	571734.934	6504996.822	97.060	0	4

Appendix 8: Illustration of deformation zones mapped by SGU, along the tunnel lining in QGis